UNIVERSITÉ PARIS SACLAY

MASTER THESIS

Optimization study: energy storage in a wave power farm

Author:
Fausto
CALDERÓN-OBALDÍA

Supervisor:
PhD. Anne BLAVETTE

A thesis submitted in fulfillment of the requirements
for the degree of Master in Science in
Renewable Energy Science and Technology

performed at

SATIE Laboratory
École Normale Supérieure de Rennes

August 21, 2016

UNIVERSITÉ PARIS SACLAY

Abstract

SATIE Laboratory

Master in Science in
Renewable Energy Science and Technology

Optimization study: energy storage in a wave power farm

by Fausto CALDERÓN-OBALDÍA

As the majority of the renewable energy sources, waves are a fluctuating resource. If a wave farm is connected to a weak electric grid, problems might emerge due to the variability of its output power profile. One of the possible problems is the increase of the Joule losses, which diminishes the overall efficiency of the farm. The main focus of the present work is to analyze the profitability of including energy storage, as a way to increase the energy production of the farm, by reduction of the Joule losses. An optimal capacity of the storage units is found, for which, an interface between a power systems software (DIgSILENT PowerFactory) and an external script written in Python is developed. This interface allows to perform an optimization process (using the Nelder-Mead algorithm) taking advantage of the capabilities of PowerFactory to perform the power flows and dynamic simulations. A comparison between a centralized and a decentralized configuration for the energy storage is also studied, with the aim to determine the best configuration for the application at stake. The evaluation of the suitability of a decentralized optimization algorithm (ADMM) for this particular case study is also presented. A summary with the main conclusions and future perspectives is developed in the last chapter of the document.

Acknowledgements

I would first like to thank the University of Costa Rica for all its support, without which, it would not have been possible to achieve the completion of this master degree.

I would also like to thank KIC InnoEnergy for giving me the opportunity to be part of its distinguished master program in renewable energy.

I would naturally like to thank my thesis supervisor, Mme. Anne Blavette of the SATIE laboratory, whose dedicated work and advice throughout the entire development of this project, made me improve significantly in my scientific skills; which will be of extreme importance in my future career.

Last but not least important, I want to thank Roman Le Goff Latimier, whose scientific advice was of a great significance as well.

Thanks to all the people: my parents, relatives and friends who, in one way or another, always gave me their support during this period of studies abroad.

Contents

List of Figures

List of Tables

List of Abbreviations

STC	**S**torage **T**ime **C**onstant
WEC	**W**ave **E**nergy **C**onverter
CS	**C**entralized **S**torage
DCS	**D**e**C**entralized **S**torage
STE	**ST**orage **E**fficiency
PF	**P**ower**F**actory
NM	**N**elder-**M**ead
DFIG	**D**oubly **F**ed **I**nduction **G**enerator
PMSG	**P**ermanent **M**agnet **S**ynchronous **G**enerator
PCC	**P**oint of **C**ommon **C**oupling
LVRT	**L**ow **V**oltage **R**ide **T**hrough

Chapter 1

Bibliographical review

In this chapter, a brief overview of the wave energy production is made, covering the most important aspects that are addressed further in this study. Characteristics of the wave resource, wave energy converters (WECs) as well as storage means typically used in wave farms are some of the topics covered in the following sections. The idea is to give the reader a minimum background to comprehend the rest of the study presented through the following chapters.

1.1 Wave energy

1.1.1 Overview

Seas and oceans are abundant sources of energy. Wind, ocean currents, tides and waves are some of the energy resources that can be found and exploited on the seas and oceans over the world. Any marine energy resource varies over time and spatially. This variation depends on several meteorological and geographical characteristics. The particular case study presented here is based on the waves as energy source, hence the review developed on this chapter is mainly focused on this resource.

The desire to exploit waves as an energy resource is not new. A French patent, dated 1799, stated the intention of the exploitation of this energy source (Multon, 2013). Waves are a by-product of the wind, which in turn is a by-product of solar radiation. The wind creates movement in the upper layer of the water in the open sea, creating small undulations that merge together to form bigger waves which travel along the ocean. The energy transported by them is the sum of their kinetic and potential energy.

1.1.2 Wave power

Wave power is defined by the flow of its total energy through a vertical surface perpendicular to the direction of propagation (Multon, 2013). If a loss-free propagation is assumed, the value of the kinetic and potential components is the same and can be written as:

$$|E_k(t)| = |E_p(t)| = \frac{\rho_w g H^2}{16} = \frac{E_m}{2} \tag{1.1}$$

where ρ_w is the density of seawater, g stands for the gravity acceleration and H is the height of the wave, from crest to trough. The velocity of propagation of the wave, assuming an infinite water depth, can be expressed as:

$$v_g(T) = \frac{gT}{4\pi} \tag{1.2}$$

where T is the period of the sinusoidal wave.

With the previous results, an expression for the power carried by a wave (per meter of wave front) can be written as:

$$P_w = E_m v_g = \frac{\rho_w g^2}{32\pi} H^2 T \tag{1.3}$$

where 1.3 is valid for unidirectional sinusoidal waves.

1.1.3 Sea state characteristics

A $swell$, is an aggregate of waves with different frequencies, phases and amplitudes. Therefore, sometimes the terms swell energy or wave energy are used as synonymous, but $swell$ stands for poly-chromatic sea-states while the term waves refers to mono-chromatic ones.

To characterize the sea state of a given geographical location, some parameters are normally used as a measure of its energetic content, taking into account its spectral profile. These parameters are:

- Significant wave height, H_s: is the mean of the highest third of the waves in a time-series of waves, representing a certain sea state.
- Wave period, T_p: is the wave period with the highest energy (Mitchell, 1999). The peak wave frequency f_p is the inverse of T_p.

The pair of parameters (H_s, T_p) define the sea state. This sea state is normally assumed stationary over a period ranging from 10 minutes to 1 hour (Multon, 2013). The sea states are normally measured using buoys that allow to generate diagrams of the probability of occurrence of different sea states in an annual basis. An example of this diagrams is shown in Figure 1.1

Then, the average annual wave power of each sea state is found as a weighted sum of the power per meter of wave front (given in 1.3) and its probability of occurrence.

Figure 1.2 shows a worldwide distribution of the wave energy resource, to have an idea of its potential in the different parts of the world. One of the main information on this map is that wave power is relatively abundant at +/-60 degrees in latitude.

1.1.4 Wave energy converters

A classification given by Falcão (Falcão, 2010), based on hydro-mechanical principles, establish the following categories of wave energy converters (WECs).

Over-topping devices

These devices have fixed structures, that allow waves to flood them increasing the water level on a reservoir, letting a water height difference when the waves back up. This water height difference can be turbined to produce

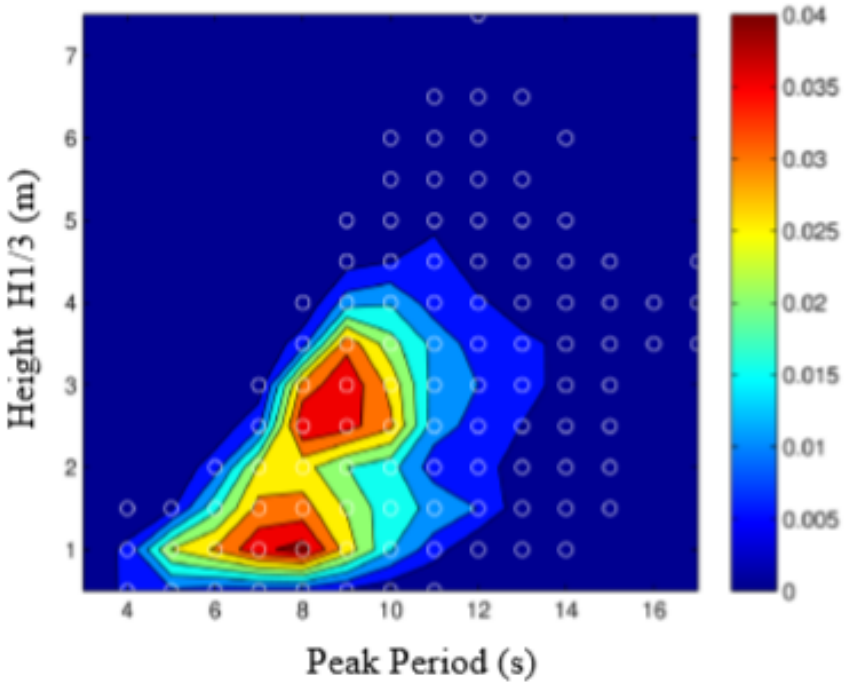

FIGURE 1.1: Probability of occurrence of different sea states, site at the isle of Yeu (*www.iste.co.uk/multon/marine.zip/ accessed* 27.7.2016).

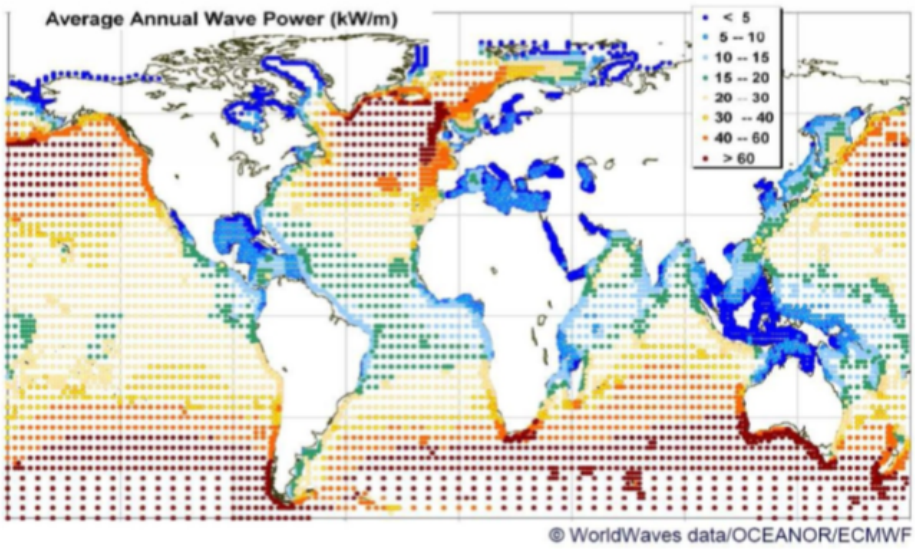

FIGURE 1.2: Worldwide distribution of the wave energy resource (*www.iste.co.uk/multon/marine.zip/ accessed* 27.7.2016).

electricity. An example of the working principle of these kind of devices is shown in Figure 1.3.

Examples of these devices are the Seawave Slot-Cone Generator in the island of Kvitsoy, Norway (*http://www.waveenergy.no/Project.htm accessed:18.7.2016*), and the Wave Dragon model of which, a testing device has been installed

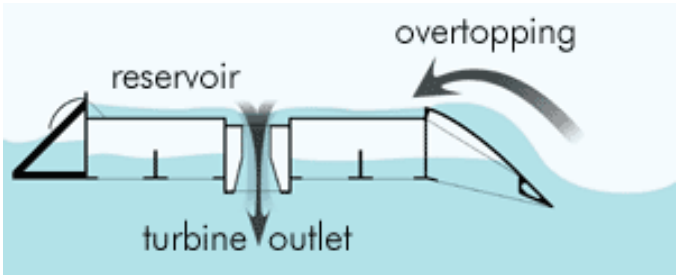

FIGURE 1.3: Working principle of over-topping systems (*www.wavedragon.net/ accessed* 28.7.2016).

at Nissum Bredning at the Danish Wave Energy Test Center in Denmark (*www.wavedragon.net/ accessed 28.7.2016*).

Oscillating water column

This type of devices exploit the changes in pressure in the air contained in a chamber, produced due to variations in the water level. The chamber has a submerged opening that connects the inside water with the sea water; then any change in the water level outside will be reflected in the inside water level as well. This variation in the water level in turn, produce an variation in the air pressure that fills the rest of the chamber. This "piston" effect is then used to move a turbine as seen in Figure 1.4.

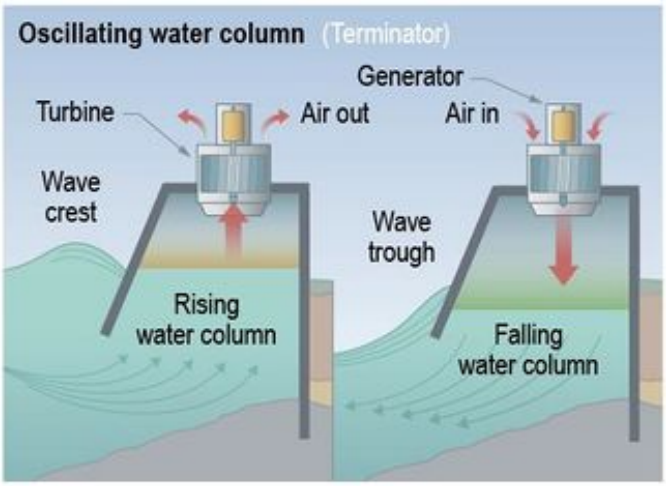

FIGURE 1.4: Working principle of oscillating water column devices.
(*http://en.openei.org/wiki/Marine_and_Hydrokinetic_Technology_Glossary accessed:28.7.2016*)

Examples of these devices are the *kvaerner column* built at Toftestallen in Norway, the *Limpet* plant in Scotland and the plant on *Pico* in the Azores islands in the Atlantic cost of Portugal (Multon, 2013).

Oscillating body systems

These devices are based on floating objects that move as the waves pass along them. The movement produced by the passing waves is transformed

to electrical energy via an electrical generator. There are different types or variations of these systems. For instance, the *Pelamis attenuator* installed in northern Portugal in 2008, consist of a series of floating cylinders linked by joints with two degrees of freedom. The relative movements induced by the waves are absorbed using hydraulic pumps and stored in pneumatic accumulators to be further transformed into electrical energy.

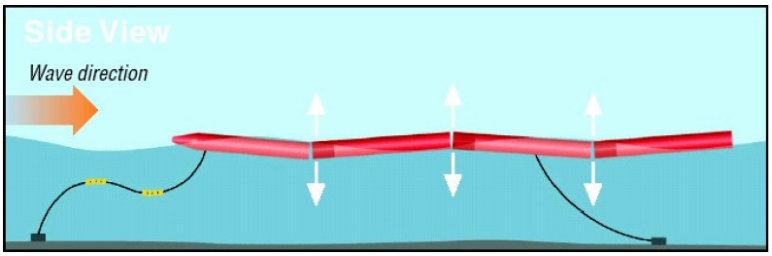

FIGURE 1.5: The Pelamis system (*http://www.esru.strath.ac.uk/EandE/Web_sites/14-15/Wave_Energy/attenuator.html accessed 28.7.2016*).

Another device that falls in this category is the point absorber. This is the type of device that is used in the present case study (particularly the semi-submerged). The size of this type of devices is small compared to the wavelength of the incident swell. In the case of semi-submerged devices, the reciprocating movements provoked by the waves passing along the floating "buoy" can be directly transformed into electrical energy using linear electric generators. An example of a point absorber is shown in Figure 1.6.

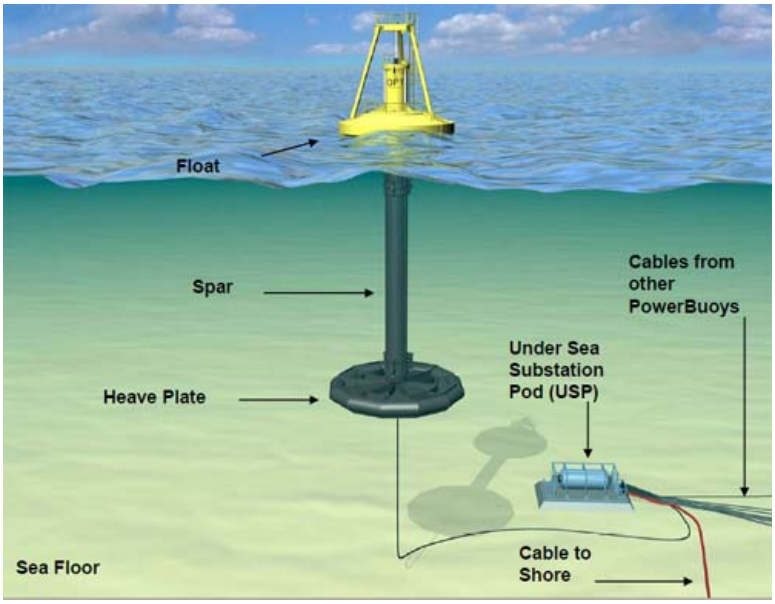

FIGURE 1.6: The point absorber system (*http* : *//oceanenergy.wikidot.com/pointabsorbers accessed* 28.7.2016).

Example of point absorber devices are the PB150 PowerBuoy, developed by Ocean Power Technologies (*http://www.oceanpowertechnologies.com/powerbuoy/*) and the *CETO* testing device developed by Carnegie Wave Energy Ltd (*http://carnegiewave.com/what-is-ceto/*).

1.1.5 Power take-off

Hydraulic

Some point absorber devices use hydraulic rams to pump an hydraulic fluid as the driving mean. This fluid is later converted to a rotating motion in a hydraulic circuit. This circuit can include accumulators and hydraulic motors. The electrical generator is directly shaft-connected to the hydraulic motor. Even when the final converting device is an electrical generator of the type mentioned in the previous sections, the presence of the hydraulic interface makes the behavior of this system different, holding some particular advantages. For instance, if significant energy is accumulated in the hydraulic circuit, the rotational speed of the generator can be significantly smoothed (Plummer and Schlotter, 2009). Besides, the smoothing capabilities provided by the hydraulic accumulators along with the inertia of the rotating parts (i.e. electric generator) gives this type of power train a smoother power output compared to a direct-drive system.

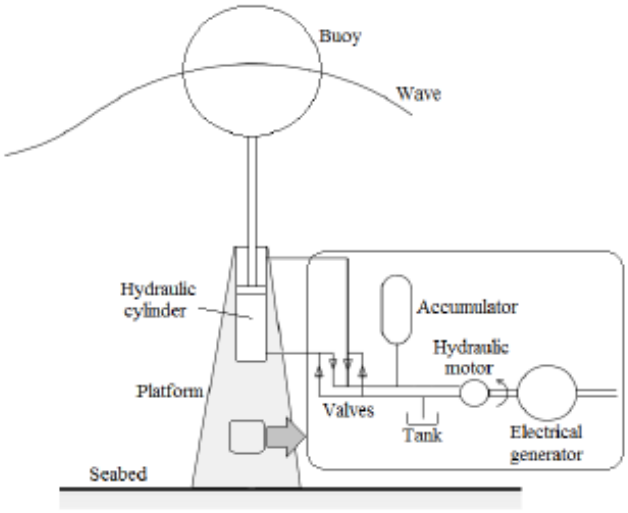

FIGURE 1.7: Hydraulic power take-off (Beirão and Malça, 2011).

Direct drive

The reciprocating motion of a point absorber can be directly connected to an electrical generator. In this case, the generator can be a direct-drive linear generator, that is able to convert directly the reciprocating movement into electricity. Another option is to have a rotary electric generator that, via some mechanisms, translate the bi-directional translation movement into a uni-directional rotational movement. In the case of a linear generator, its power take-off design has to be custom-made for the required application whereas in the case of rotary generators any induction or synchronous machine is suitable, as long as power converters are used to compensate speed variations.

In any case, the maintenance in off-shore devices has to be minimized as it is expensive and complicated due the highly energetic sea conditions of

the sites where these devices are installed. Hence, reducing the number of mechanical parts is desirable, as they require regular maintenance usually more often than electrical parts.

1.1.6 Electrical generator type

It is important to give a brief overview about the different types of generators used in wave energy systems to convert the mechanical energy coming from the waves into electricity. For this purpose, an overall classification can be made between fixed and variable speed solutions (Alcorn and O'Sullivan, 2013).

Fixed speed solutions

In this case, the generator is linked directly to the supply grid. They are usually rotary devices therefore, the angular speed of the rotor is fixed by the grid frequency, the gear ratio and the number of pole pairs of the generator. They have a simple and reliable construction, require less maintenance and are more economic. On the other hand, some of the drawbacks found for this type of devices are: low energy capture, higher mechanical stress, poorer power quality and requirement of reactive energy compensation. For these reasons, this type of solution is never used for wave energy applications. Examples of these devices are the squirrel-cage induction generator, wound rotor synchronous machine and permanent magnet synchronous generator.

Variable speed solutions

In these devices, variable speed is achieved by means of power electronics. Interfacing generators and the grid through power converters allows the generator to work at variable rotary speeds, even when the frequency of the grid is fixed. Some of the advantages of variable speed solutions are: decoupling of the grid and generator, rotor and other rotary parts can constitute a significant inertial storage capability (thus providing enhanced low-voltage ride-through capability), less mechanical stress, active and reactive power can be fully controlled and improved wave power capture thanks to a better matching between the resource and the prime mover speed. The main disadvantage is the increase of the cost due to the use of power electronics.

A typical machine used in variable speed solutions is the doubly-fed induction generator (DFIG), but permanent-magnet synchronous generators (PMSG) can be also used in a full-converter topology. DFIG topology allows variable speed operation and active and reactive power control within certain limits. However, the requirement of slip-rings is a drawback of this technology as the maintenance requirements increase. On the contrary, PMSG do not require slip-rings, they present a better control over the speed and active and reactive power are fully controlled. On the other hand, the magnets used in PMSG are very sensitive to corrosion which represents a disadvantage of these devices, besides the fact that permanent magnets are brittle so they are prone to crack under high mechanical stress.

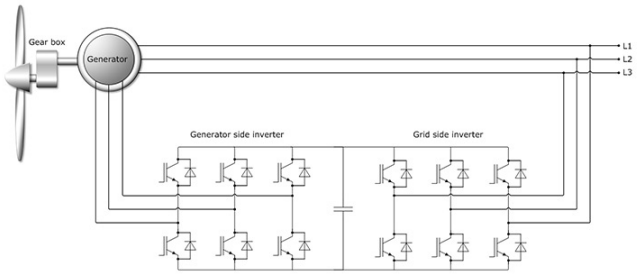

FIGURE 1.8: DFIG topology
(*https* : *//www.semikron.com/applications/wind* − *energy/application* − *examples.html accessed* 28.7.2016).

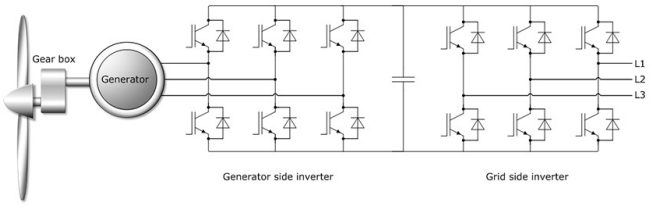

FIGURE 1.9: Full converter topology
(*https* : *//www.semikron.com/applications/wind* − *energy/application* − *examples.html accessed* 28.7.2016).

1.2 Storage for wave energy systems

In this section, an overview of some of the most commonly used storage means in marine energy systems is given. The main reasons for using storage in wave energy converters, a review of the costs and the most salient technical aspects of the different technologies are presented.

1.2.1 Motivations for using energy storage

Low-voltage ride-through (LVRT) and ancillary services

Low-voltage ride-through refers to the capability of a grid-connected installation to remain connected during low-voltage events (short circuit conditions). The use of energy storage helps to diminish the effect of such events which can cause negative effects for the consumers and the WECs. A voltage drop is a consequence of this events, then it causes reduction in the power transmission capability, therefore the WEC generator speed increases. This latter event can cause the disconnection of the WEC if speed exceeds a maximum allowed value. One way to prevent this is to store energy as inertial energy, thus reducing the speed increase, ideally leading to the speed remaining below the maximum allowed value until voltage is restored to its normal range. In this case, disconnection is avoided, which increases the stability of the power system compared to the case where installations were allowed/forced to disconnect when a fault occurred.

Besides, ancillary services inherent to any power facility such as: starting not self-starting turbines, lighting, communications and ventilation, need to be available at any moment, independently if the wave resource

is available or not. Storage help to keep these services readily available at any time when they are needed.

Power smoothing

The nature of waves is highly fluctuating and difficult to predict. The variations on the power being produced by this resource can be very high, and this could impede the connection to the main grid if the power quality requirements are not complied. Besides, if the WEC is connected to a grid with a high impedance (low short circuit power), flicker and voltage issues may arise, as the varying current from wave energy farms may affect local voltage (Alcorn and O'Sullivan, 2013).

Flicker is related to voltage amplitude variations in the supply that results in variations of the light intensity from lighting sources. This variations, if perceptible by humans, can cause headaches or visual discomfort (Wilkins, Veitch, and Lehman, 2010) and in some electronic devices can cause malfunctioning or even damage (Bollen and Gu, 2006).

The need of equipment overrating is related to the peak-to-average power output ratio, and clearly the bigger the rating the more expensive the device. This condition can be reduced if the inherent variations of the resource are smoothed by means of storage.

Moreover, due to the power fluctuations, the Joule losses of the system fluctuate as well. This cyclic heat dissipation can be harmful for equipment with different temperature coefficients and different coefficients of thermal expansion. This degrades interconnections throughout the system, for example between wire bonds and silicon in power electronic converter modules (Alcorn and O'Sullivan, 2013). Moreover, when two power sources with the same average power are compared, but one with a constant power output and the other with a fluctuating power output, there is an increase in power losses in the latter case, which can be quantified as:

$$P_{Loss} = R_{sys}\left[\frac{1}{T}\int_0^T I_{rms}^2(t)dt - I_{avg}^2\right] \tag{1.4}$$

where R_{sys} is the internal electrical resistance of the power source and T is the study period, while I_{rms} and I_{avg} stand for the instant root-mean-square current and the average current correspondingly. This increase on power losses reduces the overall efficiency of the system and might eventually cause a reduction on the profits of the farm, which is one of the subjects of study of the present project.

1.2.2 Overview of energy storage for wave energy production

In the scope of the present study, the storage is intended to reduce the power losses of a wave energy farm. This can be achieved by smoothing the rapid variations generated by wave energy converters due to the inherent fluctuations of the wave resource, as commented in previous sections. Therefore, just short-term (few seconds) energy storage systems are addressed, in particular the ones that are most promising and suitable for WEC applications in terms of performance and costs.

Figure 1.10 presents a Ragone diagram which helps to have a better overview of the different storage technologies currently available, along with their performance.

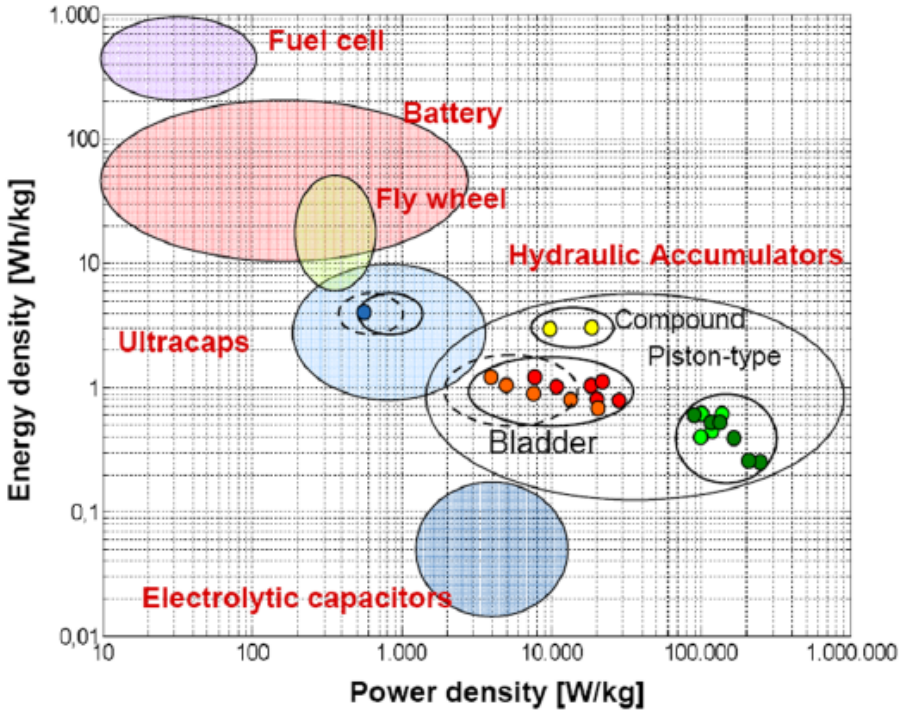

FIGURE 1.10: Ragone diagram with some of the storage technologies used in wave energy production (*https://www.researchgate.net/figure/256095814_fig1_Figure-1-Ragone-diagram-for-storage-devices-3 accessed 29.7.2016*)

Supercapacitors

Supercapacitors (SCs) are also known as electric or electrochemical double layer capacitors, since they differ from regular capacitors in the fact that, the capacitance is build up in an internal double layer. This feature allows them to increase significantly the capacitance by increasing the electrodes area by several orders of magnitude (Alcorn and O'Sullivan, 2013). The amount of energy stored by a supercapacitor can be computed as in a regular capacitor as:

$$W_c = \frac{1}{2}CV^2 \tag{1.5}$$

where C and V are the capacitance and voltage of the capacitor accordingly.

The power smoothing influence of a supercapacitor on the power output of a WEC can be modeled as a first-order low-pass filter (Santos et al., 2012) (Blavette et al., 2015) (Sullivan et al., 2010) with the following transfer function in the frequency domain:

$$\frac{V_{out}}{V_{in}} = \frac{1}{1 + RCs} \tag{1.6}$$

where $\tau = RC$ is the time constant of the filter, R being the internal resistance of the SC and C its capacitance. V_{in} and V_{out} are the input and output voltages of the SC respectively. s is the Laplacian frequency variable. The time constant of a SC is typically in the order of seconds (Alcorn and O'Sullivan, 2013).

Some of the most salient characteristics of supercapacitors are listed below (Luo et al., 2015) (Chen et al., 2009a):

- Large specific power (up to 10 kW/kg)
- High cyclability (more than 100 000 cycles)
- Broad working temperature range (-40°C to 65°C)
- Fast charge/discharge (1 – 10 seconds)
- High cycle efficiency (84–97%)
- Low maintenance

Some particular drawbacks of supercapacitors, compared to other storage means such as inertial storage or batteries are (Luo et al., 2015) (Chen et al., 2009a):

- Low specific energy ($\approx$ 2.5-15 Wh/kg)
- Low cell voltage ($\approx$ 2.7V)
- Linear voltage variation during discharge (implies the use of power electronics to control it)
- High daily self-discharge rate (up to 40%)

Inertial storage

Inertial storage stands for any medium that is able to store energy in the form of kinetic energy; they are normally considered as short-term energy storage means. In the case of rotating devices, the energy they can store/deliver during the change between two different rotor speeds ω_1 and ω_2 can be obtained as:

$$W_{inertia} = \frac{1}{2} J(\omega_1^2 - \omega_2^2) \tag{1.7}$$

Where J is the moment of inertia that depends on its physical characteristics (mass and geometry).

Any rotational device (such as a turbine or a rotatory electric generator) has already an intrinsic inertia, hence they already have some built-in energy storage capability. However, it is important to mention that not all WECs have turbines or rotatory electric generators (i.e. WECs with linear generators such as the Seabased device developed by the University of Uppsala, Sweden (Danielsson, Eriksson, and Leijon, 2006).

Some of the salient points of inertial storage are (Luo et al., 2015):

- Turbines, motors and generators already have flywheel effect, which diminishes the amount of extra-storage needed

- Highly reliable
- Long service life (15-20 years)
- Cycle efficiency (90-95%)
- Reasonable specific energy for short term applications (5-80 Wh/kg)
- Almost no derating of the storage capacity as a function of time
- Quick charge time

Some of the disadvantages of inertial storage are (Luo et al., 2015):

- Size and weight
- Maintenance Required
- Low specific power (0.4 – 1.5 kW/kg)
- Rotating speed variation during "charge/discharge" which implies the use of power electronics to keep a constant voltage

Hydraulic accumulators

Among hydraulic accumulators, hydro-pneumatic storage is the most commonly used in wave energy devices. It usually has a pressure storage reservoir in which a non-compressible hydraulic fluid is held under pressure by an external mean. The external mean can be a spring, a raised weight or a compressed gas (*www.hydraulic-equipment-manufacturers.com accessed 29.7.2016*).

This method normally has a high pressure accumulator that combines a fluid and a gas, which provides the energy storage capability. Hence, the actual storage mechanism is a compressed gas (normally dry nitrogen (O. Falcão, 2007)) that absorbs/delivers directly the stored energy into the hydraulic fluid, which will later move the hydraulic motors to produce electricity.

The energy that can be stored and transferred during gas expansion-compression (assuming an isentropic process) is given by:

$$W_{gas} = mc_v(T_{emp_1} - T_{emp_2}) \tag{1.8}$$

where m is the mass of the gas, c_v is the specific heat at constant volume, T_{emp_1} and T_{emp_2} are the absolute temperatures in Kelvin before/after expansion. These temperatures can be related with the pressure of the gas using the ideal gas law:

$$PV = nRT_{emp} \tag{1.9}$$

where P is the absolute pressure, V is the volume, n is the number of moles of gas, R is the ideal gases constant and T_{emp} is the absolute temperature.

Some of the salient points of this type of energy storage are (Pourmovahed et al., 1988) (Pettersson and Tikkanen, 2009):

- Long lifetime (more than 20 years or 15 000 cycles)
- High cycle efficiency (up to 90%)

- High power density (up to 100 kW/kg)

Some of the drawback for this type of storage are listed below (Lemofouet and Rufer, 2006) (Pettersson and Tikkanen, 2009):

- Low energy density (1-2.5 Wh/kg)
- High volume for long-term storage applications

A summary of the most salient technical features of the three types of storage means presented in this section is shown in Table 1.1 (Luo et al., 2015) (Chen et al., 2009a) (Chen et al., 2009b) (Pourmovahed et al., 1988) (Lemofouet and Rufer, 2006) (Rastler, 2010).

TABLE 1.1: Technical features of storage means for wave energy production

	Hydro-pneumatic(HYPES)	Inertial (flywheel)	Super capacitors (SCs)
Energy density (Wh/L)	-	20-80	10-30
Power density (W/L)	-	1000-2000	100000
Specific energy (Wh/kg)	1-2.5	10-30	2.5-15
Specific power (W/kg)	100000	400-1500	500-10000
Daily self-discharge (%)	-	100 (>20% per hour)	10-40
Lifetime (years)	20+	15-20	10-30
Cycling times (Cycles)	15 000	20000	100000
Discharge efficiency (%)	-	90-93	95-98
Cycle efficiency (%)	Up to 95	90-95	84-97
Response time	Seconds-minutes	Seconds (1cycle)	Milliseconds (1/4 cycle)
Discharge time@ rated power	-	8s-15s	1min

Storage costs

A review of costs of the three storage means presented in the previous section, is shown in Table 1.2. The table refers to the capital costs in terms of energy, power as well as the operation and maintenance costs (Luo et al., 2015) (Chen et al., 2009a) (Rastler, 2010) (Kondoh et al., 2000) (Lemofouet and Rufer, 2006).

TABLE 1.2: Capital and operation & maintenance costs of different storage means.

	Power Capital Cost (US$/kW)	Energy Capital Cost (US$/kWh)	Operating and Maintenance Cost (US$/kW/year)
Hydro-pneumatic(HYPES)	495-6600	85-1100	660-1650
Inertial (Flywheel)	250-350	1000-5000	20
Super Capacitors (SCs)	100-300	300-2000	6

1.3 Motivation for the study

The power fluctuations in a wave farm may deteriorate significantly the power quality in the local networks to which they are connected (Blavette et al., 2014). In this particular paper, Blavette et al. investigates the issue of the grid impact of a wave farm in terms of flicker. In a further paper (Blavette et al., 2015) she tackles the storage sizing issue for a wave farm, with the

aim to reduce the flicker levels in the local network; however, neither of them address the problem from an economical point of view.

Some other research works have tackled some economical considerations for marine energy converter farms (Nambiar et al., 2015). Nambiar et al. focus on a techno-economic analysis framework to assess different transmission options for marine energy converter farms. On the technical front, they analyze the feasibility of the transmission option considering supply quality constraints and the optimal sizing of reactive power compensation to allow maximum real power transfer capability. The economic viability of different transmission options is measured based on component costs and the costs associated with losses. However, even when they include the cost of Joule losses during power transmission as part of the techno-economical study, they never address the issue of how to reduce these losses or the eventual effects that storage might have on them either.

Santos et al. (Santos et al., 2012) do actually tackle the benefits of storage in a wave farm using point absorber arrays regarding the improvement of power quality. They perform an interesting study for the AMETS site in the coasts of Ireland, using comprehensive information about the sea states on this site; they tackle the effects of short-term storage for power smoothing of the power profile for wave farms connected to local grids. However, the effects studied are focused on the smoothing effect that storage has in power and voltage variations as well as the reduction in flicker levels on grids with different strengths. Once again, the economical assessment of the inclusion of storage in the wave farm, is left apart. Even when the results show a positive effect in terms of power smoothing, it remains unknown if, from an economical perspective, it is viable or not to include the storage.

Hence, the present study aims to tackle a particular issue that has not been addressed so far. This refers to the direct effect of storage in a wave energy farm, in terms of reduction of Joule losses and its consequent repercussions in terms of economical benefits. The idea is to perform an optimization process in which, the optimization variables are the time constant of the storage units (proportional to its storage capacity) and where the objective function is the variation on annual profits of the farm.

The study then mixes a technical component, which is the expected reduction on joule losses when storage is placed, as well as the economical side which studies whether the technical benefits of placing the storage pay off the investment.

This optimization is carried out using a novel approach in which a power systems software (DIgSILENT PowerFactory *http://www.digsilent.de/ accessed:15.8.2016*) is used along with an external optimization algorithm to evaluate the objective function. The development of the interface that allows such communication between PowerFactory (PF) and the optimization script (written in Python) is another of the main outcomes of the present project. This interface opens the possibility of further use of PowerFactory to perform customized optimization, which is a not built-in feature in the software.

Chapter 2

Preliminary study on power losses

This preliminary study is carried out with the aim of comparing and validating the results obtained by the optimization method presented in Chapter 4 and deciding which configuration is more suitable for the application at stake. The idea is to study the effect of the time constants of the storage over the power losses of the farm by both, a centralized and a decentralized storage configuration. In the following sections, the different simulations performed are presented as well as the results and some important implications.

2.1 Model

2.1.1 DIgSILENT PowerFactory

DIgSILENT PowerFactory is a power system analysis software designed for applications in generation, transmission, distribution and industrial systems. The name DIgSILENT stands for "DIgital SImuLation and Electrical NeTwork calculation program". It has been designed as an advanced integrated and interactive software package dedicated to electrical power system and control analysis in order to achieve the main objectives of planning and operation optimization. DIgSILENT Version 7 was the world's first power system analysis software with an integrated graphical one-line interface. That interactive one-line diagram included drawing functions, editing capabilities and all relevant static and dynamic calculation features ($www.digsilent.de$).

It utilizes the Newton-Raphson algorithm to solve power flows calculations (Gonzalez-Longatt and Rueda, 2014) and has a comprehensive library where a wide variety of models of typical power system elements can be found. For this study, three-phase (AC, 50 Hz) balanced conditions are considered and RMS simulations are performed. The built-in static generator model is used to model the wave energy converters and the storage units. A static generator is a generic model of an electrical generator available in PowerFactory to simulate different renewable energy sources and/or energy storage. Submarine cables and transformers are chosen from the built-in library of the software. Their parameters are inherited from the previous studies where this model was taken from.

2.1.2 Layout of the farm

The present work is based on previous studies performed by Blavette et al. (Blavette et al., 2014) (Blavette et al., 2015); therefore, the model of the wave farm used has been based on these previous works. The layout of the system is presented in Figure 2.1.

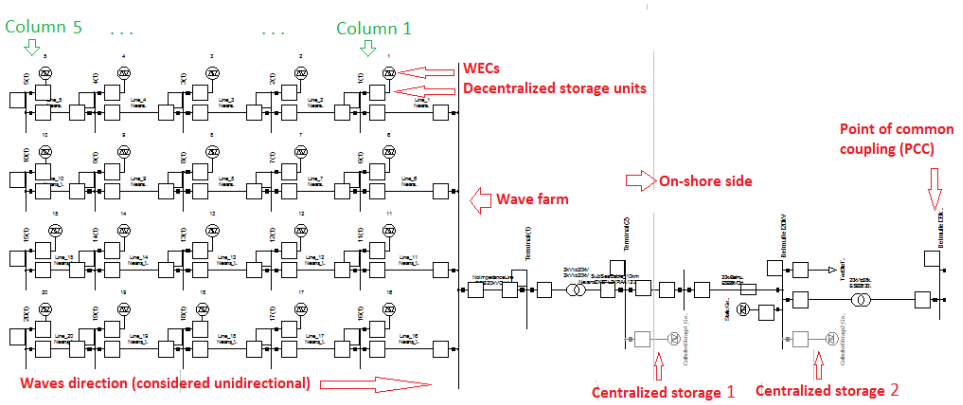

FIGURE 2.1: Farm layout (PowerFactory model).

In this model, the wave energy converters (WECs) are represented by static generators. There are also two static generators simulating storage units that are placed in the on-shore section of the farm. All these units can be activated or deactivated at will, allowing to test any storage configuration desired. The direction of the waves is assumed to be perpendicular to the columns of WECs, as depicted in Figure 2.1. This assumption is rather ideal, as in real conditions the waves normally approach the array from different directions. Under this assumption, a time delay is included to model the spatial separation between WECs. In this case, the separation is considered only between the columns of WECs, as it is considered that each wave hits all the WECs of one column at the same time. This assumption reduces the "aggregation effect" (explained later in this chapter) as there are just 5 blocks of WECs working alternatively, instead of 20 (which would be most likely the case in real conditions).

2.1.3 The power profile

It is important to know the output power profile of the WECs used to perform the simulations presented in this chapter. It is very irregular as depicted in Figure 2.2; but is considered periodic over its time duration. This means that, for this case study, the same power profile is repeated every 700 s. As any periodic signal, it could be decomposed in a sum of harmonic components (sinus and cosine functions) according to the Fourier theory as:

$$f(t) = \frac{a_0}{2} + \sum_{n=1}^{\infty}(a_n \cos \omega_n t \; + \; b_n \sin \omega_n t) \tag{2.1}$$

where a_0, a_n and b_n are the Fourier coefficients and ω_n is the n_{th} harmonic frequency.

The total power transmitted by this signal is therefore, the sum of the power contributions of each of its harmonics. Hence, filtering some of these

harmonic components (as the storage model does) would result in a decrease on the power carried by the signal after passing the filter. This effect could be small assuming that the mean-component a_0 is far bigger than its harmonics a_n, b_n. In any case, it is something to take into account in case a deeper analysis were to be performed. In real conditions this phenomena would not occur, as a storage unit would always "give back" the energy it stores. Therefore, it is expected that the results of energy production of the present study, could be smaller than the ones expected in real conditions.

It is considered in this work, that there is no limitations on the energy capacity of the storage; any value can be chosen. However, for the sake of simplicity the study is restricted to values in the range of 5 seconds, as from previous studies this range shows the highest impact on losses reduction, hence it is considered sufficient to attain the objectives.

Figures 2.2 and 2.3 present the power profile utilized in the present study over a 700 second period as well as a zoom-in over a 20 second period accordingly.

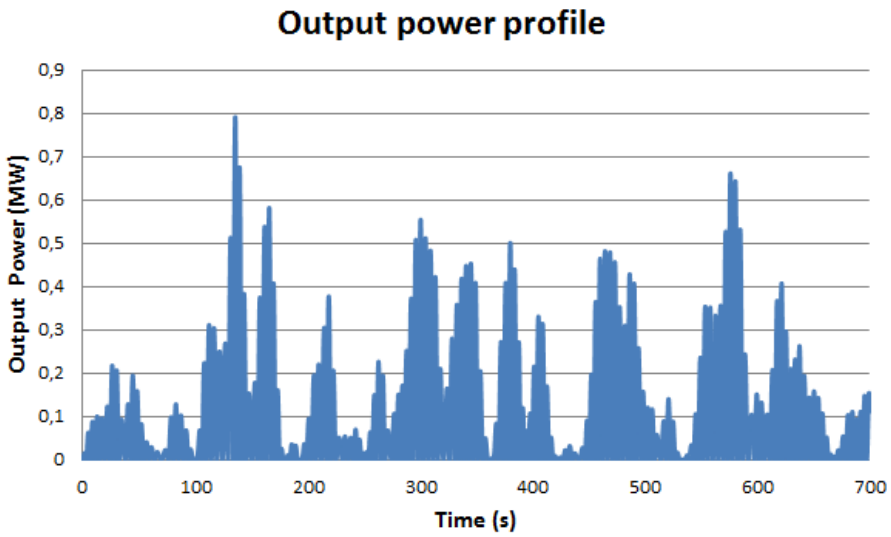

FIGURE 2.2: Output power profile of one WEC

In order to model the physical separation between the WECs in the wave farm, a random time delay t_{di} is used. All WECs are considered to have the same output profile as the one depicted in Figure 2.2, but it is randomly displaced according to t_{di}. Figure 2.4 presents the power profiles of the WECs corresponding to column 1 and column 2 of the array according to Figure 2.1. As previously mentioned in Section 2.1.2, this assumption is quite ideal, as in real conditions this would not be the case. As water is a dispersive medium, waves of different frequencies do not travel at the same speed; hence, WECs located at different places along the wave propagation line would have different profiles. However, not using this approximation would require computing the sea elevation in every point where a WEC is located, as well as computing also their hydro-mechanical behavior and the inter-WEC interactions. Moreover, the approximate approach presented earlier is considered as sufficient in a large number of studies focusing on electrical engineering purposes (Blavette et al., 2014), (Santos et al., 2012) (Blavette et al., 2015), hence, this approach was also adopted in this work.

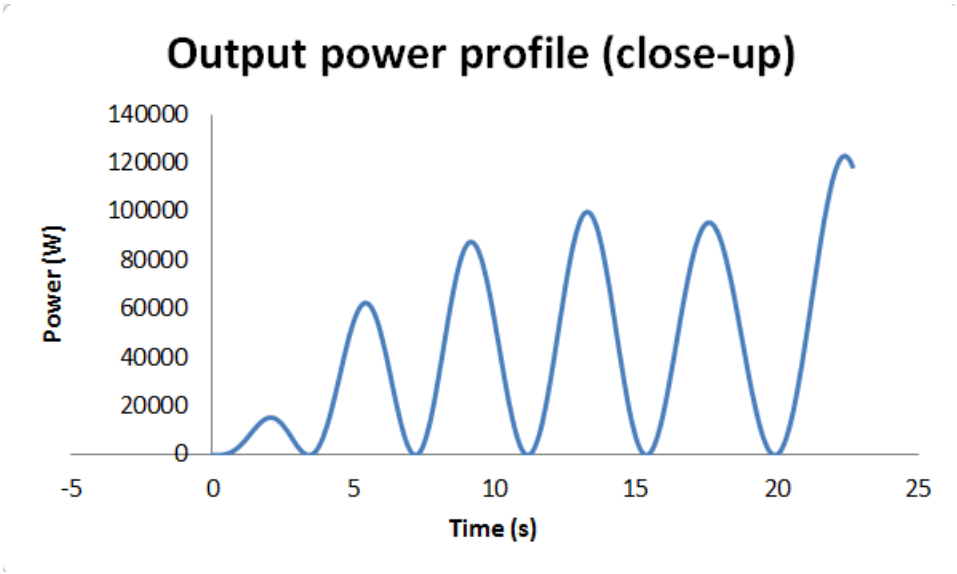

FIGURE 2.3: Output power profile of one WEC (close-up over a 20 second period).

The physical idea behind the inclusion of this time delay t_{di} is to include in the model the time that takes a wave to reach the different "columns" of the WECs array, as seen in Figure 2.1.

In order to perform the preliminary study in a reasonable period of time, the same time constant τ is set (in each simulation) for the entire array of offshore storage units (each one belonging to an specific WEC). From now on, the set of all these storage units will be called: "decentralized storage".

For the case study analyzed over the following chapters, the sea state is characterized by wave peak period of T_p = 9s and a wave significant height of H_s = 3m.

2.1.4 Storage

All the storage units are modeled as first order low-pass filters, as it has been widely used in the literature (Blavette et al., 2015) (Santos et al., 2012) (Sullivan et al., 2010). Therefore, this model was selected by my supervisor herself, as the selection/development of storage unit models is out of the scope of this internship. However, further work are on-going in the SATIE research center to investigate the suitability of this model for real-case storage means. Storage units are considered to have a particular cycle efficiency K.

As stated in Chapter 1, supercapacitors represent the cheapest storage mean suitable for the application at stake among the three presented in Table 1.2. Besides, they have a high smoothing capability with respect to wave-induced power fluctuations due to their high power absorption/injection capability, in a context where small energy capacity is sufficient (Lemofouet and Rufer, 2006)(Abedini and Nasiri, 2008)(Abbey and Joos, 2007). For the above reasons, the present work will be based on super capacitors only. Figure 2.5 shows a simplified circuit of an ideal (100% cycle efficiency) low-pass filter using a capacitor .

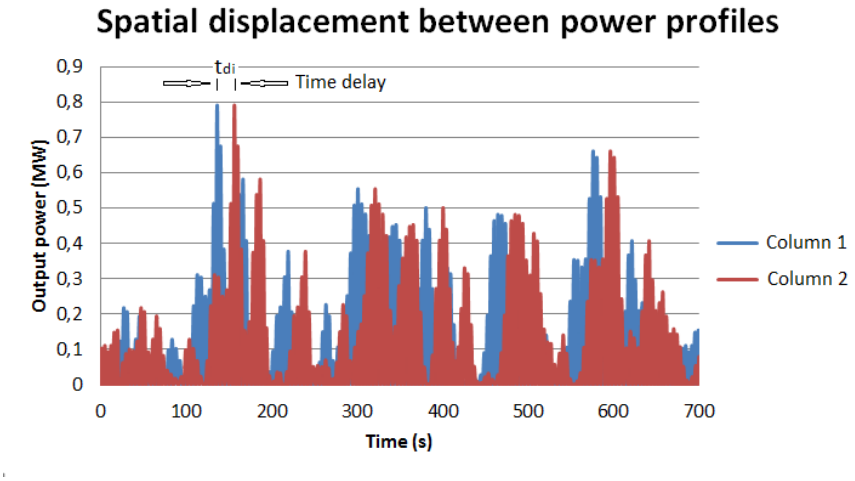

FIGURE 2.4: Example of shifting between power profiles of WECs in columns 1 and 2 of the array due to the random time delay.

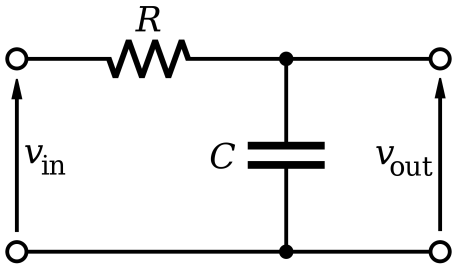

FIGURE 2.5: Simplified circuit of an ideal RC low-pass filter.

The model hereby presented is a single-line diagram, but it can perfectly be extended to a three-phase system, as in the case of the wave farm under study.

From the basic theory of electric passive filters (Williams et al., 2006), the transfer function (relation between input and output signals) in the frequency domain for the filter shown in Figure 2.5 can be written as:

$$H(s) = K \cdot \frac{1}{1 + \tau s} \tag{2.2}$$

where K is the gain of the filter, $\tau = RC$ is the time constant (in seconds) and s is the complex frequency (in radians per second). Comparing this results with a real supercapacitor bank and the model used in PowerFactory, the gain K would represent the cycle efficiency, R stands for the internal series resistance ESR of the supercapacitor bank, while the magnitude of s represents the frequency of the input signal. Therefore, the time constant could be expressed as:

$$\tau = ESR \cdot C \tag{2.3}$$

This relation is used in the following section to derive a relation between the cost of the storage and the time constant.

It is worth to mention that, storage is supposed not to alter the hydromechanical behavior of the WECs, therefore their response to waves remains unchanged as a function of τ. This seems a reasonable assumption given that the storage units to be used (supercapacitors) have a little weight compared to the weight of the WEC and its platform.

2.1.5 Methodology

Centralized vrs decentralized simulations

The models presented in the previous section were included in a PowerFactory model in order to perform the simulations. As the first step, a script was written in Matlab that is able to add up the losses in all the lines to obtain the total losses of the farm. At each simulation, this script was used to collect the data and create the graphs presented in the following section.

After that, a common value for the time constant and the cycle efficiency is set to all WECs. One set of storage (centralized 1, centralized 2, decentralized) is activated while the other two are deactivated. In this way, a dynamic simulation is performed for each value of K (K=0.9;K=0.93;K=0.96;K=1), for each value of time constant (from 0 to 5 seconds) and for each storage set independently. From each simulation, the data is collected and the graphs generated using the script. The results from the three different storage sets is merged in one graph for the sake of clearness and easiness to compare the results.

Aggregation effect simulations

In order to analyze the aggregation effect of WECs, two simulations were performed, one with just one WEC working and the second one with four WECs working. In the latter case, an average losses per WEC is obtained to be able to compare it with the first case (one WEC). In both cases, all the WECs have the same distance to the collecting point so the only variable in study is the aggregation of units. That is the reason why the comparison is made between generators on the same "column" of the array (units 1, 6, 11 and 16 in Figure 2.1). Mixing WECs from different "columns" in the array would yield inaccurate results of the variable in study.

A sweep over the values of the time constants (from 0 to 5 seconds) is performed for the decentralized storage and for K=1, as it was sufficient to achieve to objectives of this section.

Electrical distance simulations

Four WECs, at the same distance respect the collecting point, are activated at a time. In this particular case units corresponding to columns 1 and 5 (see Figure 2.1) are used to carry out the simulations. Hence, the values obtained are the addition of the effects of the four units. Dynamic simulations are run activating each set of units one at a time and for the different values of time constants (from 0 to 5 seconds). Then the total losses of the farm are computed and plotted in normalized and absolute values.

Given the little influence of the collective storage on the total losses as found in Section 2.1.6, the analysis of the electrical distance is performed only taking into account the decentralized storage units. Moreover, a cycle

efficiency K of 100% for the storage units is considered in this case to make sure the only variable under study was the electrical distance.

It it reasonable to think that there will be differences in the optimal storage time constants between WECs that are located at different distances from the collecting point. This hypothesis is addressed in Section 2.3.

2.1.6 Results

Separate sweeps for the time constants are performed independently for the: centralized storage 1, centralized storage 2 and the decentralized storage. When one of these storage sets is being studied, the other two sets are disabled (no storage considered for them).

For this study, the storage time constants (STCs) are discrete, with values ranging from 0 s to 5 s with a step size of 0.5 s. These values are arbitrarily chosen as they are sufficient to achieve the objectives proposed for this section of the study. Using the PowerFactory software, a time series simulation is run over a period of 700 seconds.

The active power losses were computed subtracting the active power flowing in both nodes of each line (the ends of each line). In this way, the difference between both values should account for the Joule losses in the line. The active power in every node of the systems is computed when a power flow is performed.

The results file contains the active power losses (Joule losses) for each line of the model and they are stored in an external file using an automated script. These values are further processed using a script written in Matlab to obtain the total losses of the farm, for each time constant and for each storage set (decentralized storage, centralized storage 1, centralized storage 2). This process is repeated for different values of the storage efficiency, namely: K=0.9, K=0.93, K=0.96 as they are typical values for supercapacitors, as stated in Table 1.1.

Simulations were also performed for K=1 to use it as the reference maximum value. The results of these simulations are shown in Figures 2.6, 2.7, 2.8 and 2.9 and Table 2.1.

The corresponding storage efficiency must be taken into account when performing the economical analysis. This cycle efficiency K is not a variable that can be deliberately chosen since it is inherent to the storage technology used due to its physical properties.

2.1.7 Results discussion

A sharp difference can be observed in Figure 2.6 regarding the effects over the total losses of the study case grid, between centralized and decentralized storage configurations. The effect of the centralized storage is negligible compared to the effect of the decentralized configuration and it is almost independent of the time constant value. This is a common point on the rest of the simulations as can be seen in Figures 2.7, 2.8 and 2.9, hence the reason why the analysis performed in Chapters 3 and 4 is focused on the decentralized storage only. This would imply that the Joules losses occur in the offshore section of the grid, hence, the onshore collective storage units have far less influence for reducing the power losses than the offshore units.

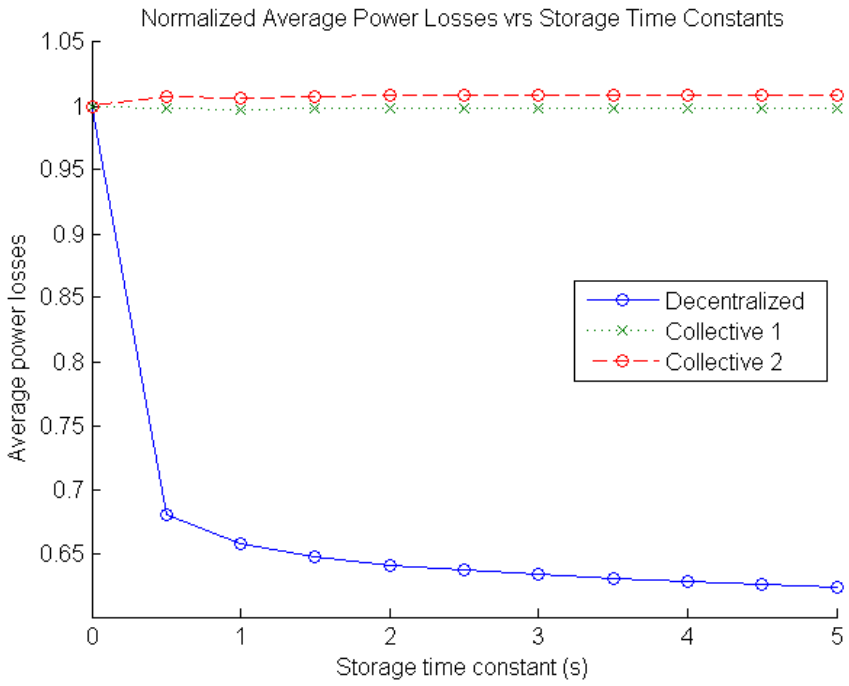

FIGURE 2.6: Normalized average power losses for K=0.9.

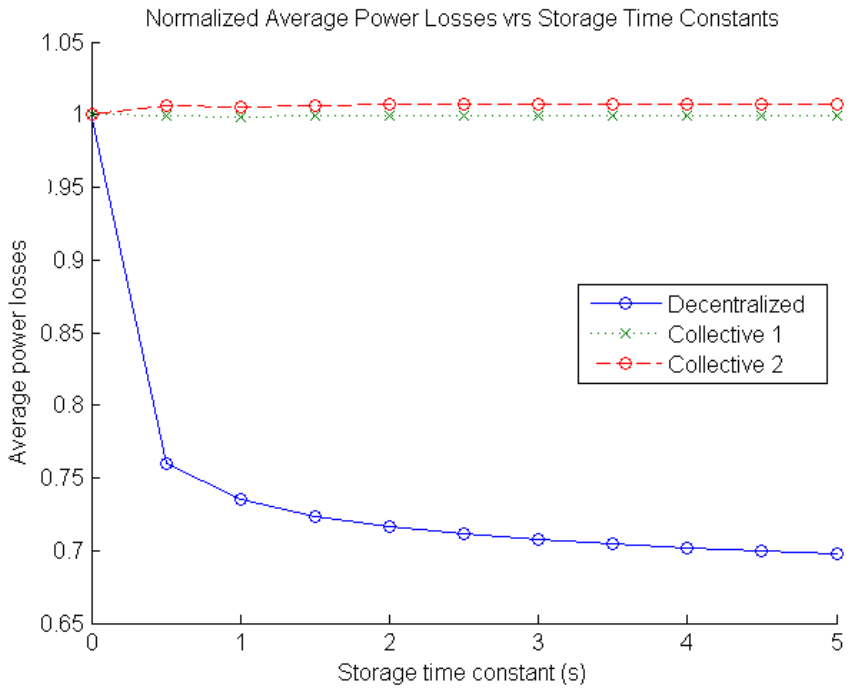

FIGURE 2.7: Normalized average power losses for K=0.93.

Besides, centralized storage units are in a higher voltage section of the farm's grid. Current levels are smaller in this section (percentage-wise respect to the cable nominal capacity), hence it is reasonable to expect smaller Joule losses in this part of the grid.

An interesting common result is the slight increase on power losses when collective storage 2 is active, as can be seen in Figures 2.6 to 2.9. These

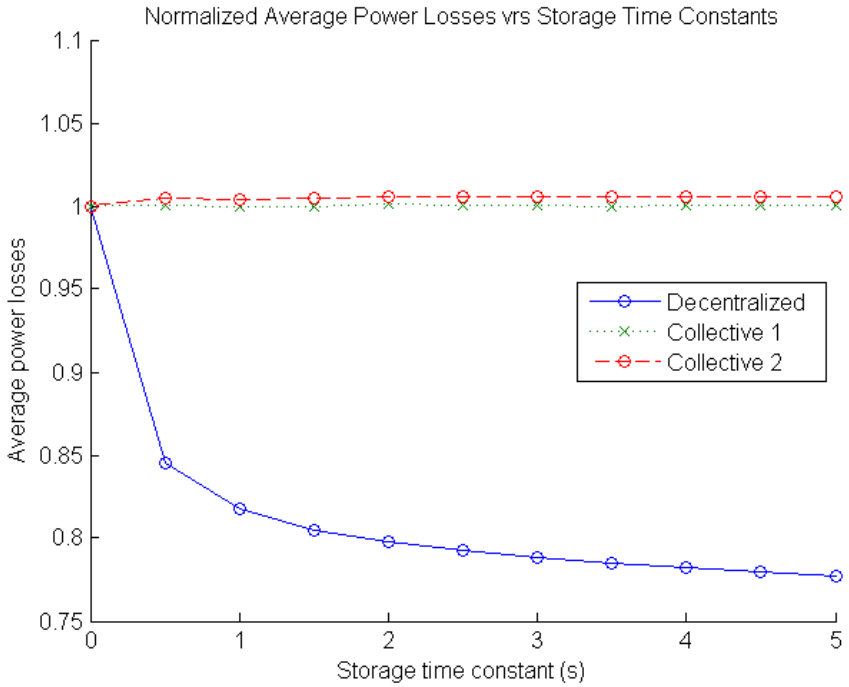

FIGURE 2.8: Normalized average power losses for K=0.96.

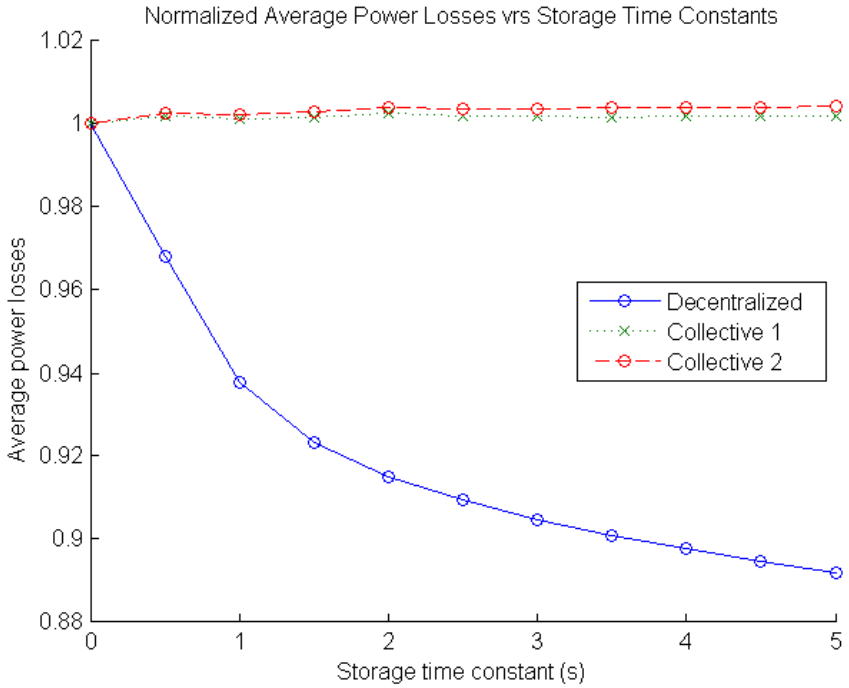

FIGURE 2.9: Normalized average power losses for K=1.

could have different reasons: one possible explanation could be that it is result of software accuracy in the convergence of the algorithms used to perform the power flows. The rate of increase in power losses is very small(< 1%), making this possibility feasible. The other possible explanation is that, as commented in a previous paragraph, storage is acting as a filter eliminating some of the components of the original signal, which in turn, reduces

its power content. This yields a loss of power in the bus where the storage is connected. This does not happens in real life as storage gives back the energy it retains, but it is not the case in the filter model being used in this work.

It was also found that active power losses of the farm strongly depend on the value of the storage efficiency (K). For instance, in the case of K=0.9, the reduction on the losses by placing a storage with a STC=0.5s is around 32%. Passing from a STC=0.5 s to STC=1 s yields an extra decrease of 2.5%. In other words, placing a storage with a STC=0.5 s provokes the highest reduction in energy losses (compared to the non-storage case). Further increments of the STCs above 1 s provoke a very small decrease in power losses (less than 1%), as seen in Figure 2.6.

On the other hand, for K=1 the reduction on the average power losses for a STC=0.5 is just 3.2%. Moreover, the reduction of passing from a STC=0.5 s to a STC=1 s is around 3%. It can be noted that, the reduction of losses when placing a storage with STC=0.5 s is ten times smaller than the analogous case for K=0.9. From this numbers, it is clear that the cycle efficiency K of the storage units plays an important role on the total losses of the farm.

This phenomena is an important point to consider in order to avoid self-deception during the optimization. As the efficiency of the storage decreases, the power flowing through the lines decreases proportionally, which means that storage units waste some energy. Hence, the losses are less but this happens at the expense of a waste of energy. This implies that, a further multi-objective optimization procedure (including costs, revenues and losses) should be performed to assess the adequacy of the storage. This procedure is presented in Chapter 4.

Therefore, if compared to the case of STC=0 s where no storage is considered, the big decrease observed in Figure 2.6 for a STC=0.5 s is due to the proportional decrease on the power flowing through the lines when a storage efficiency K (less than 100%) is included. This effect can be seen in Figure 2.10.

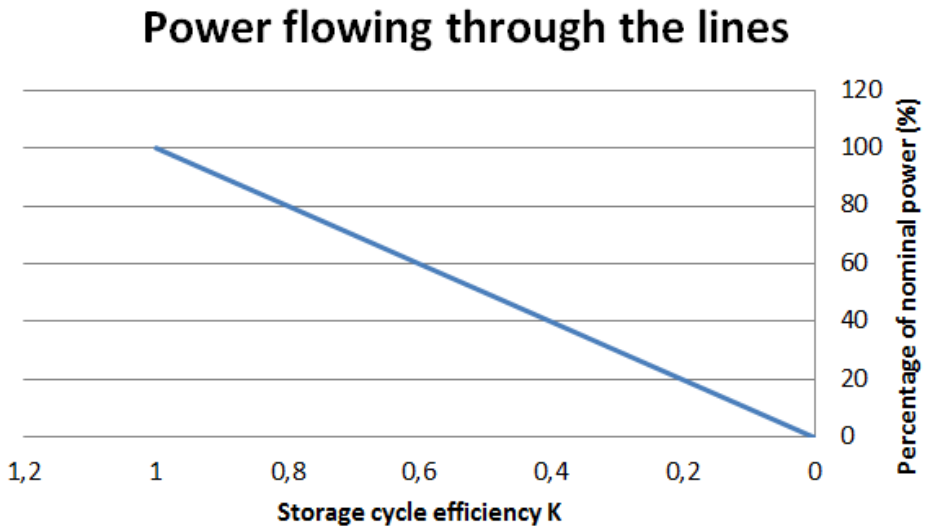

FIGURE 2.10: Power flowing through the power lines vrs the storage efficiency K according to the filter model used in this study.

Hence, simulations showed previously reflect an added effect of: the filtering of the storage plus the effect of its power losses (due to an efficiency less than 100%).

In the case of Figure 2.9 it is assumed an efficiency K of 100%. Hence, this graph shows uniquely the real filtering effect of an ideal storage unit. Figures 2.7 and 2.8 are simply intermediate cases between the cases for K=0.9 and K=1 presented in Figures 2.6 and 2.9 respectively. It is observed that these figures confirm the tendency commented in the previous paragraphs (almost no effect of collective storage over the losses).

As a side-note, it is worth to mention that the highest reduction of losses occurs for storage time constants below 1 s, which makes reasonable to think that the optimal capacity of the storage units would correspond to a time constant in this range, as it presents the best "capacity/performance" ratio.

To summarize the effect of the storage efficiency in the average total losses of the farm, Table 2.1 is presented. The values shown represent an average obtained for time constants varying from 0 to 5 seconds.

TABLE 2.1: Effect of storage efficiency in the average total losses of the wave farm.

Storage Efficiency(K)	**Average total losses(MW)**	**Average total losses(%)**
1.00	0.33	100.0
0.96	0.29	88.4
0.93	0.26	80.4
0.90	0.24	73.0

As seen in Table 2.1, for a value of K=0.9, the total losses of the farm reduces in approximately 27% due to the addition of the losses on each storage unit.

The information presented in Table 2.1 must not be misunderstood; the reduction on the losses due to a storage efficiency less than 100% is not completely "beneficial", as it reduces the final output power of the farm at the same time.

In order to have a more objective analysis, it is better to study the final output power of the farm, on the collecting point, as a function of the time constants and efficiency of the storage units, as seen in Figure 2.11. The data shown is obtained directly from simulations performed using PowerFactory.

From Figure 2.11, it is seen that the average output power at the collecting point of the farm, decreases as the efficiency K of the storage decreases, as expected. The gross profits of the farm are computed in an annual assuming a price of energy of 29.5 €/MWh. In fact, it is observed that for any efficiency(K) less than 96% the power losses provoked by the storage efficiency surpass the reduction in power losses due to the filtering effect of the storage. This yields a lower output power compared to the case when no storage is placed.

As conclusion from the results previously presented, it can be summarized that:

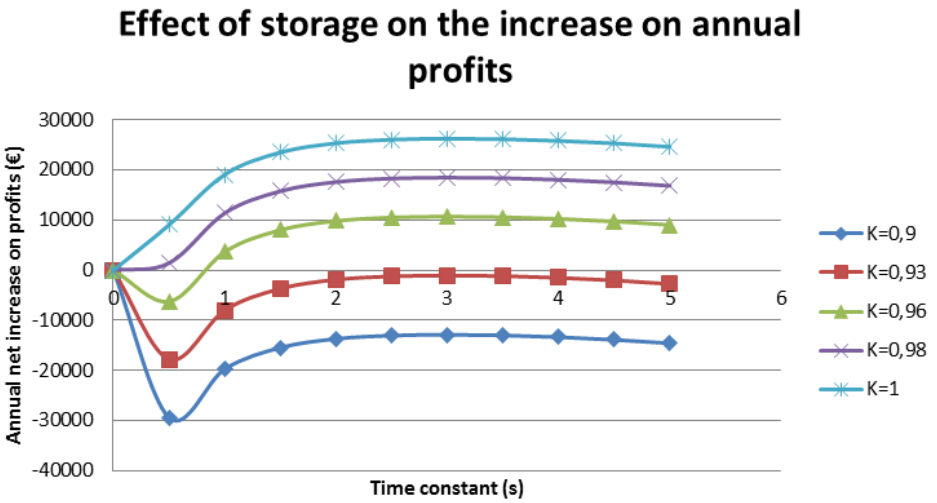

FIGURE 2.11: Output power of the farm as function of time constants and efficiency of the storage units

- For an storage cycle efficiency (K) less than 96% , placing storage provokes more losses than "savings" in terms of output power, which in turn reduces the total power output of the farm.
- Centralized storage has no positive effect in reducing active power losses, while decentralized storage does have an effect that depends on the value of time constant chosen. Values of time constants less than 1 second present the highest reduction on power losses.

2.2 Effects of aggregation on power losses

In this case study, aggregation stands for the effect of having several WECs generating power simultaneously, with output power profiles that are displaced in time by a random delay. Since the output power profile of each WEC is irregular due to the intrinsic nature of the energy source (irregular waves), the superposition of the output of several devices working in parallel might have an effect on the total losses by lowering peak-to-average ratio of the profile. The output power profile of the farm, that results from the superposition of the 20 WECs is presented in Figure 2.12. Figure 2.13 shows the peak-to-average ratio in the output power of the farm of one WEC compared with 20 WECs. Here, the effect of aggregation is clear as it reduces this parameter when 20 WECs are used.

After computing the results, a slight decrease of 0.5% in the total losses of the farm is found for the case of having four WECs compared with the case when only one WEC is working. It is reasonable to think that this should be the expected behavior due to the aggregation effect, that results in a decrease of the Joule losses. However, for the size of the case study wave farm, this effect is quite small (less than 1%), hence, it could be reasonably neglected. Results are shown in Table 2.2.

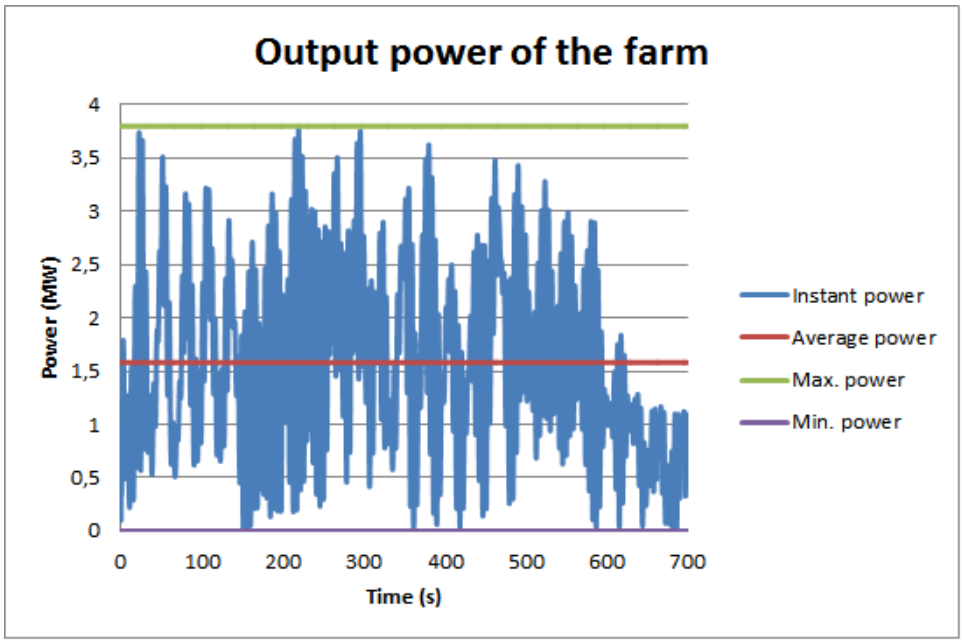

FIGURE 2.12: Output power profile of the farm.

TABLE 2.2: Summary of aggregation effect on farm's losses

Average Loss per WEC(MW) 1 WEC	Average Loss per WEC(MW) 4 WECs	Difference(%)
0.015802	0.015714	0.55

2.3 Effects of Impedance on power losses

In Figure 2.14, a model of a transmission line that is typically used in power systems analysis called PI model is presented, where the different components of its impedance can be identified.

The parameters R, L, C depend on the physical length of an electrical conductor (among other aspects). Therefore, the total impedance of a cable or a transmission line depends, to an important extent, on its length. In this case study, all impedances are measured with respect to the PCC (see figure 2.1).

From the basic theory of electrical circuits it is known that the Joule losses in an electrical conductor follow the next relation:

$$P = I^2 * R \tag{2.4}$$

where I is the current flowing through an electrical conductor and R is its resistance.

The current I in equation 2.4 is proportional to the impedance according to Ohm's Law. Therefore, as R, L, C depend on the length of the cables, Joule losses are directly affected by this parameter, hence the reason of this section of the study. The model of the cables utilized by PowerFactory take into account all these effects (series inductance, parallel capacitance and series resistance), therefore the results obtained take into account (implicitly) all these effects.

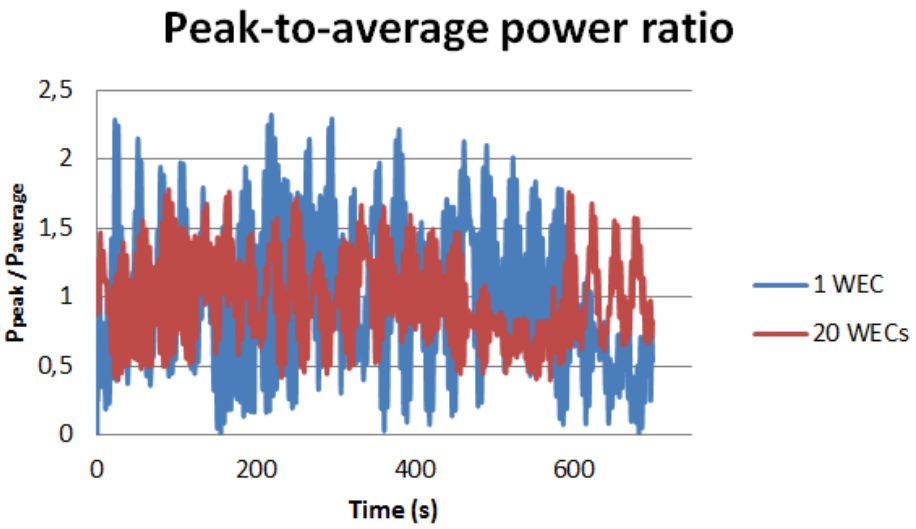

FIGURE 2.13: Peak-to-average ratio of the farm comparing 1 WEC against 20 WECs.

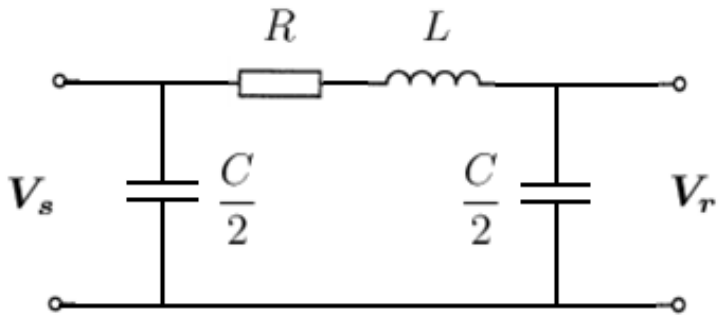

FIGURE 2.14: PI model of a transmission line (http://www.openelectrical.org/ accessed:10.8.16).

In Figure 2.15, the normalized power losses for the first column of WECs as function of the time constant τ is presented. This column is the one that has the shortest distance to the point of common coupling (PCC). In this case, for a time constant of five seconds, the power losses reduce up to a 65% of the value with no storage. In absolute terms in column 1, the reduction when passing from no storage to a storage with a time constant of five seconds is 6.2kW, as seen in Figure 2.16.

In Figure 2.17, the normalized power losses for the column 5 of WECs as function of the time constant τ is presented. This column has the longest distance to the PCC. In this case, for a time constant of five seconds, the power losses reduce up to a 71.6% of the value with no storage. In absolute terms in column 5, there is a decrease of 17.8kW when passing from a time constant of zero second (no storage) to a time constant of five seconds. This is almost three times higher than the reduction obtained in the first column, under the same conditions. This effect can be observed in Figure 2.18.

Comparing the two cases between columns one and five, we can conclude that the effect of placing storage on column five (longest distance)

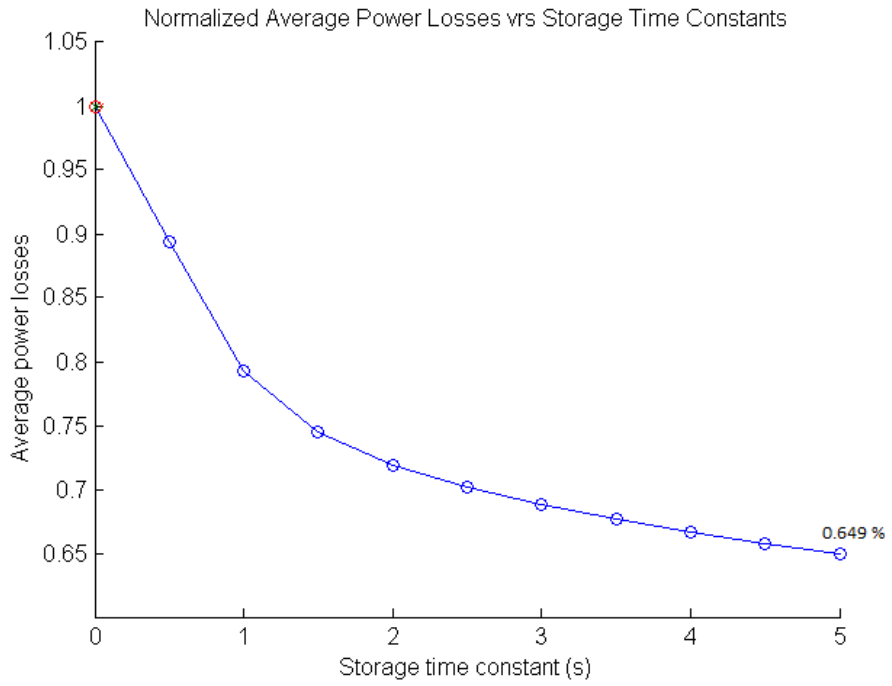

FIGURE 2.15: Normalized power losses for units in column 1 (decentralized storage).

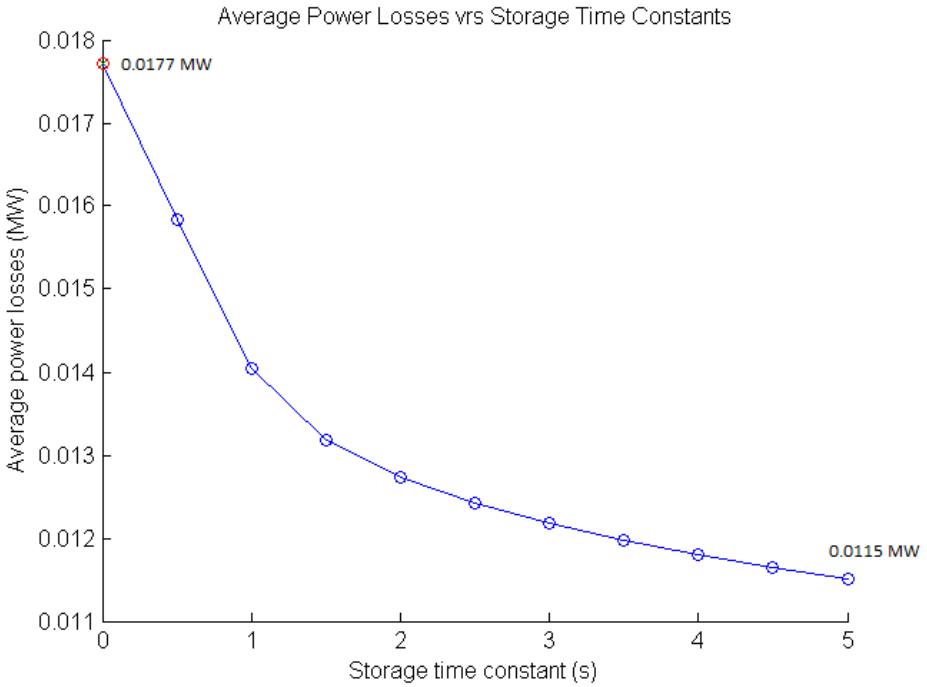

FIGURE 2.16: Absolute power losses for units in column 1 (decentralized storage).

is stronger (2.87 times) in terms of reduction of the losses, than the corresponding for column one (shortest distance), as expected. If a ratio is computed of how big the storage should be (value of time constant) in order to

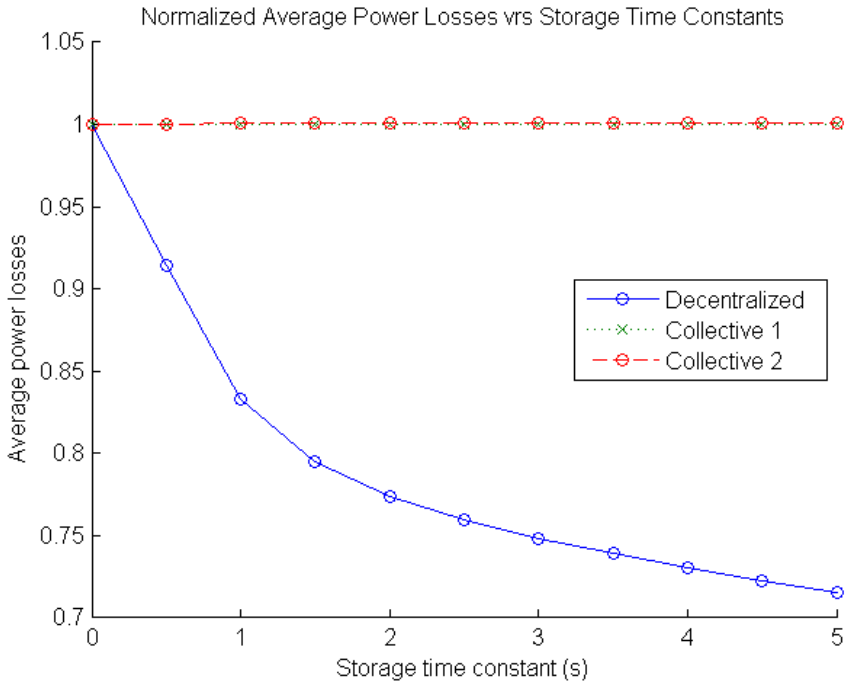

FIGURE 2.17: Normalized power losses for units in column 5

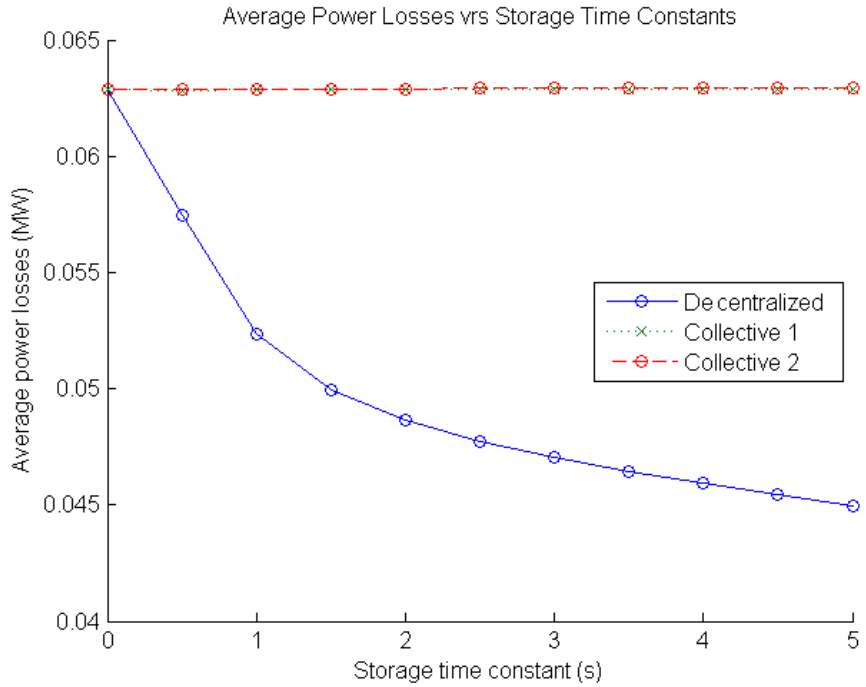

FIGURE 2.18: Absolute power losses for units in column 5

reduce one kilowatt of losses; values of 0.80 s/kW and 0.28 s/kW for storage placed in columns one and five are obtained. Putting it inversely, for every "second of storage" (second in the time constant of the storage) placed in columns one and five, a reduction of 1.25kW/s and 3.57kW/s is obtained respectively. In simple words, it is worth more to place storage in column

five than in column one as the reduction in losses achieved is bigger. A summary of the results explained in previous paragraphs is presented in Table 2.3.

TABLE 2.3: Effect of electrical distance over the average power losses of the farm.[1]

	Loss reduction(kW)
Column 1	6,2
Column 5	17,8

Therefore, after the optimization, it is reasonable to expect a decrease of the optimal size of the storage units as the distance from the PCC decreases. In other words, it would be reasonable to expect storage units with bigger time constants in column five than the ones in column one. This hypothesis is studied in Chapter 4 where the optimization results are presented.

[1]Reduction corresponding to a variation of the time constant from 0 to 5 seconds accounted for 4 WECs.

Chapter 3

Optimization problem

It is opportune to recall at this point, what is the final aim of the optimization problem for this particular case-study. In plain words, the objective is to find out whether the annual-net-profits of the farm increase by placing storage; and if it does, find out the capacity of the storage that yields the maximum increase.

In this chapter, the optimization problem to be addressed in the rest of the present study is formulated. In order to attain this goal, other ancillary developments are carried out as well, such as the procurement of a relationship between the costs of the storage and its time constant. In this case, only super capacitors are considered for the reasons explained in Section 2.1.4 and confirmed by the results presented in Section 2.1.6.

The work developed in this chapter serves as a prelude for the optimization study presented in Chapter 4.

3.1 Optimization problem

3.1.1 Overview

The idea of the optimization, is to use the features of PowerFactory for power flows and dynamic simulations in conjunction with an external optimization algorithm. Basically, it is necessary to develop a script that is able to perform the optimization procedure (with any suitable algorithm) that can, at every iteration, retrieve the value for of the energy production using storage ($E_S(\tau)$) from the dynamic simulation in PowerFactory. In this case, it is not necessary to develop an explicit function for $E_S(\tau)$ and the energy production without storage (E_{NS}), as they can be computed directly from the PowerFactory results.

This avoid the need of computing derivatives, which could become time consuming if a high number of variables is used. Besides, some of the models that PowerFactory includes, are developed directly by the manufacturers of the equipment based on experimental tests. Therefore one could expect its results to be more accurate than the ones one could achieve by developing a mathematical model "by hand" using generic models of the components.

Another advantage of using PowerFactory is its graphical interface, which makes the construction of a power system rather intuitive and fast. Modeling by hand a power system of a high number of buses can become complex and the chances of making mistakes are higher. Its versatility for setting and changing the parameters make it also very suitable for try-and-error approaches, when the test of different scenarios is desired. Figure 3.1 shows

a diagram sketching the working flow of the theoretical and the PowerFactory approaches, where the differences between the two can be noted more easily.

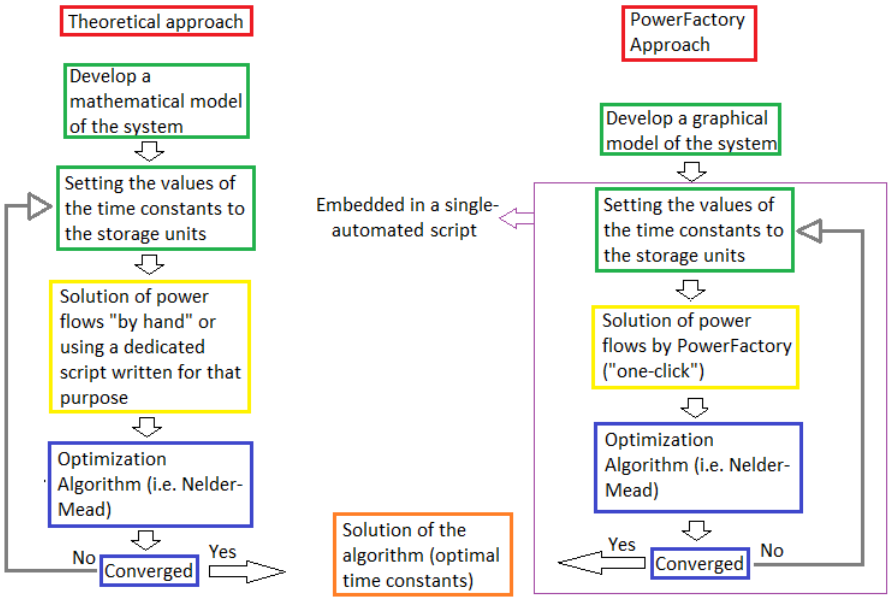

FIGURE 3.1: Diagram showing the differences between theoretical and PowerFactory approaches.

If the evaluation of Equation 3.1 yields a negative value of $P_{profit}(\tau)$, it means that including storage produces losses to the farm with respect to the no-storage case. In such case, it makes no sense to place storage. On the other hand, if $P_{profit}(\tau)$ yields a positive value, it means that there would be an increase on the annual profits if storage is installed. The time constant of this storage would be retrieved from the optimization algorithm.

In Chapter 4 the implementation and results of this optimization procedure are presented in detail.

3.1.2 General formulation

In order to evaluate the increase on the profits, due to the use of storage, it is mandatory to compare the performance of the farm with respect to the case where no storage is used. So the problem at stake is to maximize the increase of profits of the farm (if there is any), which can be written as:

$$P_{rofit}(\tau) = [E_S(\tau) \cdot E_c - S_c(\tau) - \Delta P_c(\tau)] - [E_{NS} \cdot E_c - \Delta P_{c_{NS}}] \quad (3.1)$$

where τ is a vector containing the time constants for all the WECs of the farm and is the optimization variable. P_{profit} represents the net variation in annual profits when storage is used (compared to the no-storage case) while $S_c(\tau)$ is the cost of the storage installed. The procurement of $S_c(\tau)$ is developed in Section 3.2. $\Delta P_c(\tau)$ is the cost of power fluctuations when there is storage present while $\Delta P_{c_{NS}}$ is the reference cost of power fluctuations when no storage is used. Their derivation is described in Section 3.3. The values for $E_S(\tau)$ and E_{NS} are found running a dynamic simulation

with the software Powerfactory for the study case farm. Based on its power output results, the energy can easily be computed over the desired study period. The function given by 3.1 depends also on the value of the cycle efficiency K of the storage, but in this case study this parameter is fixed to a value of $K = 0.96$, considered to be a representative average value for supercapacitor banks (as stated in Chapter 1).

3.2 Storage cost function $S_c(\tau)$

In order to obtain the function of the cost of the storage $S_i(\tau_i)$, it is necessary to obtain a mathematical relation between the time constant and the dynamical characteristics of the storage mean. For the purpose of this study, only supercapacitor banks are considered since, as seen in Chapter 1, it is the cheapest storage-mean from the three means studied for this application. After having this first correlation between the time constants τ and the parameters that determine the dynamic behavior of the storage (such as the capacitance on a supercapacitor bank), a further relation between the latter and the energy-and-power characteristics of the storage mean has to be further developed to be able to relate the price of the storage with the time constants τ. These steps are developed on the following sections.

3.2.1 Relation between cost of storage and its time constant

As mentioned in Chapter 1, the cost of storage means are given in terms of energy and power. In this section, an approach that takes into account both, energy and power, is addressed with the aim to develop a relation between the cost of storage and the time constant which is required for the optimization procedure.

For the sake of simplicity and time constraints for the completion of this project, only a capacitor bank is analyzed. But clearly, a similar development can be followed with different storage-means (i.e. Inertial-flywheel) in order to obtain a relation between its cost and the corresponding time constant.

From basic electric theory it is known that the energy stored in a parallel-plates capacitor can be expressed as:

$$E_C = \frac{1}{2} \cdot C \cdot V^2 \tag{3.2}$$

where C is the capacitance and V is the voltage at which the capacitor is working.

Power is a rate of how fast energy is delivered (or absorbed) expressed as:

$$Power = \frac{\Delta E}{\Delta t} \tag{3.3}$$

where Δt is the time during which the energy ΔE is delivered.

In the particular case of a capacitor according to 3.3, the power it should withstand will be dictated by the energy that it has stored (or has to store), and the period of time during which that amount of energy needs to be delivered or absorbed.

As in the present study, the capacitor is being used for power smoothing, it is desired that it has the ability to deliver all its energy as fast as the power "spike" occurs (as a worst-case scenario), so it can completely "smooth" the output. In Figure 3.2 a zoom-in on the power profile used in this case study for the WECs is presented to realize the duration of the power "spikes". From this figure it can be seen that the power variations or "spikes" have an average duration of 2.5 seconds.

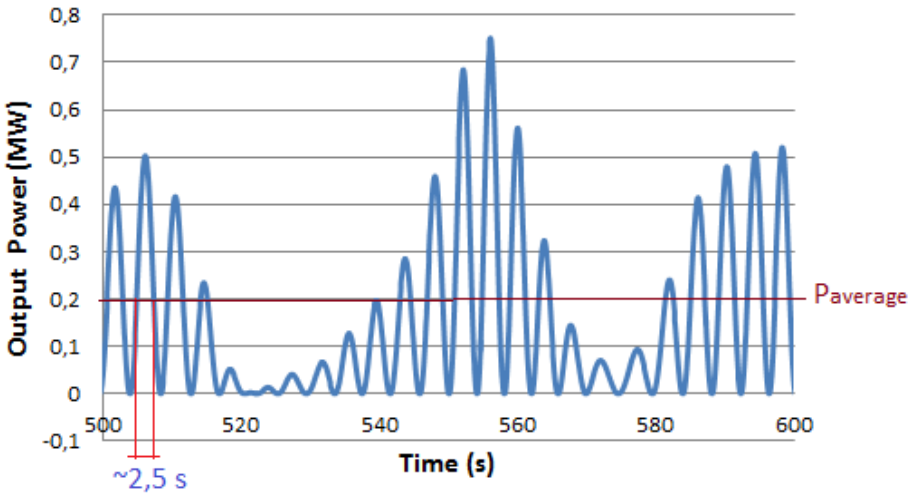

FIGURE 3.2: Power variations in a study-case power profile of a wave energy converter.

If the capacitance C, is solved in terms of the time constant τ from equation 2.3, and replaced in 3.2 it is obtained:

$$E_C = \frac{1}{2} \cdot \frac{\tau_i}{ESR} \cdot V^2 \tag{3.4}$$

where ESR is the equivalent series resistance of the capacitor.

Assuming the "worst-case-scenario", when the storage has to deliver/absorb the maximum amount of energy it can handle, using 3.4, the equation 3.3 can be rewritten as:

$$P_i(\tau_i) = \frac{ESR \cdot V^2 \cdot \tau_i}{2\Delta t} \tag{3.5}$$

where the subscript i stands for the i_{th} storage unit.

If a price for the power of a capacitor bank P_c is given (in €/W), then the capital cost of each storage unit, as a function of its time constant, could be expressed as:

$$S_{c_i}(\tau_i) = P_c \frac{ESR \cdot V^2 \cdot \tau_i}{2\Delta t} \tag{3.6}$$

which is the general relation required in Section 3.1 for the optimization.

In Chapter 1, average prices for different storage means are presented in terms of energy and power. An extract of this information with capital costs for super-capacitor banks is presented in Table 3.1.

[1]References can be found in chapter 1

TABLE 3.1: Average capital costs for super-capacitor banks.[1]

Price per Power (US$ / kW)
100-300

If SI units are used in 3.4 for the time constant and ESR, the resultant energy is given in Joules. Using the conversion factor $1\ kWh = 3.6.10^6\ J$, the results of Table 3.1 for P_c (an average value of 200 $US\$/kW$ is adopted), a value of $ESR = 240m\Omega$ (Maxwell, 2015), a value of $\Delta t = 2.5\ s$ as stated in Figure 3.2 and a working voltage of V=400V (as used in the PowerFactory model); equation 3.6 can be evaluated and rewritten as:

$$S_{c_i}(\tau_i) \approx 1359 \cdot \tau\ (€) \tag{3.7}$$

where a exchange rate of $1.13\ US\$/€$ is used($www.fxtop.com/\ accessed$: 4.5.2016).

As equation 3.7 expresses the capital cost, it is useful to compute an annual cost for economical analysis. Assuming a lifetime of 10 years (Kovaltchouk, 2015) and a typical (annual) interest rate of 6% (IEA, 2016), the annual cost per storage unit can be obtained using the following relation:

$$C_{annual} = \frac{r \cdot C_{capital}}{1 - (1+r)^{-y}}\ (€/year) \tag{3.8}$$

where $C_{capital}$ is the capital cost, r is the interest rate and y is the number of years (useful life of storage). With this result, the cost of a storage unit obtained in equation 3.7 can be rewritten in an annual base as:

$$S_{c_i}(\tau_i) \approx 191 \cdot \tau\ (€/year - unit) \tag{3.9}$$

The previous relation is used in Chapter 4 to perform the optimization procedure.

3.3 Power variations cost function $\Delta P_c(\tau)$

The cost of the variations of power is a very subjective topic so far, as there is no straight-forward rules, or international regulations for its definition. As an example, the impact on power quality that a highly variable power profile could have in a small island, where the grid is weak, would be much more noticeable and problematic than the same case where the production farm is connected to a large-strong electric grid. Besides, the characteristics of the consumers of the electricity, dictates also how problematic would be to have variations in the power supply. The sensitivity of the industrial processes to power fluctuations varies depending on the type of activity as well as the potential economic repercussions derived from these fluctuations.

In most of the countries the voltage levels are restricted to a range of values. For instance, in the United Kingdom, voltages must be kept withing a range of +10%-6% according the British Standards Institution on its policy "Nominal voltages for low voltage public electricity supply systems" (BSI,

2015). Flicker is another parameter that is already restricted by most countries. In Europe, the standards IEC61000-3-3 and IEC61000-3-11 dictate the limits over this parameter. In this sense, power variations are already indirectly limited by regulations. However, grid compliance does not prevent significant power variations from occurring, which can represent a certain economical burden such as the need of spinning reserve, include storage and accelerated aging of power components, among others.

As a general approach to assign a cost to this parameter, an analysis based on the day-ahead market is proposed. Supposing that the owner of a wave energy farm (or any renewable intermittent source), sells its energy to an energy market that works under the day-ahead scheme. Under this scheme, producers and consumers have to express, one day in advance, their power production/consumption for the next day. Producers will offer an average value of power they can sell over the next day (or part of the day). Then, the grid operator will count on this power "promised" by producers to satisfy the needs of the consumers.

In a real case, for a given sample period, there will be deviations on the power production from the "promised" profile expressed by the producer. If the producer is delivering more power than what he offered, assuming ideal conditions, the grid operator will not need this extra energy as all the needs of its customers are satisfied; then the producer will loose this energy. In the case producer is delivering less power than what he promised, he will have to buy this lacking energy from someone else to comply with the grid operator. As energy has a price, the producer will loose an amount of money equal to the cost of this lacking energy he has to buy to satisfy his promised production. This, would be the cost that power fluctuations (deviations from the "promised" profile) have for the producer.

It is worth to clarify that in some countries, penalties are also charged for getting rid of any surplus energy, for instance in Denmark (http://energinet.dk/DA/Sider/default.aspx accessed:12.8.2016).

Assuming this penalty is implemented, deviations are averaged over a period of time T (in hours) assuming an energy price $E_c(€/MWh)$, then the cost of the power fluctuations can be written as:

$$\Delta P_c(\tau) = F_{ave}(\tau) \cdot P_{ave}(\tau) \cdot T \cdot E_c \ (€) \tag{3.10}$$

where $P_{ave}(MWh)$ is the average power or "predicted power" of the producer which is the value promised to be delivered to the grid ahead the actual delivery. This parameter is obtained by the producer based on historic data of the resource along the year. The time period T is chosen to be one year for the reasons explained in Section 4.4.1.

F_{ave} is the average power deviation or deviation respect to the average power, normalized respect to the average power. Equation 3.11 is used to compute this parameter.

$$F_{ave}(\tau) = \frac{1}{N} \sum_{n=1}^{N} \|P_n - P_{mean}\| \tag{3.11}$$

where N is the number of time steps of the study period, P_n is the "instantaneous" power in the n_{th} time step and P_{mean} is the average power.

Equation 3.10 is an input to the objective function 3.1 expressed in Section 3.1. This objective function is used in Chapter 4 to perform the optimization procedure using the PowerFactory approach.

Chapter 4

Optimization

In this chapter, the optimization process followed to find the optimal value of the time constants of the storage units is presented. An explanation of the method, algorithm and models used is given, as well as the assumptions and limitations encountered. An analysis of the results obtained is carried out to evaluate their validity and significance. Finally, a brief explanation is given about the ADMM optimization method and why it is not suitable in the present study.

4.1 Nelder-Mead algorithm

4.1.1 Motivation

As the idea in the present study is to use PowerFactory software to perform the power flows and dynamic simulations, a suitable algorithm to perform the optimization is needed. This algorithm needs to comply with an important requirement: it should work without the need of an explicit objective function, without the need of computing its derivatives but only using the values returned by the function for a given variables set. This requirement arises from the fact that, the objective function of the problem at stake, is based on power flow computations performed by PF. Hence, the explicit mathematical model used by PowerFactory to solve this problem is not available, only its results. This force us to seek for an optimization algorithm that can work based only in the evaluation results of the objective function.

4.1.2 The algorithm

Nelder-Mead algorithm (NM) is a numerical method used to find the minimum or maximum of an objective function in a multidimensional space. It is usually applied to non-linear optimization problems for which derivative may be not known (Nelder and Mead, 1965). Nelder–Mead in n dimensions maintains a set of $n + 1$ test points arranged as a simplex. The simplest approach is to replace the worst point with a point reflected through the centroid of the remaining n points, and so the technique progresses until reaching convergence. A good definition of how the algorithm works is given by Tribbey (Tribbey, 2010):

> The downhill simplex method now takes a series of steps, most steps just moving the point of the simplex where the function is largest ("highest point") through the opposite face of the simplex to a lower point. These steps are called reflections, and

> they are constructed to conserve the volume of the simplex (and hence maintain its non-degeneracy). When it can do so, the method expands the simplex in one or another direction to take larger steps. When it reaches a "valley floor," the method contracts itself in the transverse direction and tries to ooze down the valley. If there is a situation where the simplex is trying to "pass through the eye of a needle," it contracts itself in all directions, pulling itself in around its lowest (best) point.

As any heuristic search method, Neldear-Mead can converge to local optimal points which is something to take into account when using these type of techniques (Kolda, Lewis, and Torczon, 2003).

4.1.3 Implementation

The optimization algorithm was implemented in Python. This programming language was chosen due to its compatibility for interfacing with PowerFactory. A built-in interface in which Python can be used has indeed been included in the latest releases of this software. The Nelder-Mead variation implemented for the present case study can be described in the following steps (Boyd et al., 2011):

1. Ordering.
$$f(x_1) \leq f(x_2) \leq ... \leq f(x_{n+1})$$
where $f(x_i)$ represents the objective function evaluated over the $x_{i_{th}}$ sample.

2. Computation of the centroid x_o of all points except x_{n+1}

3. Reflection. Computation of the reflected point x_r.
$$x_r = x_o + \alpha(x_o - x_{n+1}) \ (\alpha \geq 0)$$
if $f(x_1) \leq f(x_r) \leq ... < f(x_n)$, x_{n+1} is replaced by x_n and the algorithm start again from step 1.

4. Expansion. if $f(x_r) < f(x_1)$, the expanded point x_e is computed.
$$x_e = x_o + \gamma(x_r - x_o) \ (\gamma > 0)$$
if $f(x_e) < f(x_r)$, x_{n+1} is replaced by x_e; otherwise is replaced by x_r and return to step 1.

5. Contraction.if $f(x_r) > f(x_1)$, the contracted point x_c is computed.
$$x_c = x_o + \rho(x_{n+1} - x_o) \ (0 < \rho \leq 0.5)$$
if $f(x_c) < f(x_{n+1})$, x_{n+1} is replaced by x_c and go back to step 1, otherwise continue to shrink.

6. Shrink. Substitute all the points except the best point by:
$$x_i = x_1 + \sigma(x_i - x_1)$$

And go back to step 1. α, ρ, γ and σ are respectively the reflection, expansion, contraction and shrink coefficients. Standard values are $\alpha = 1$, $\gamma = 2$, $\rho = 0.5$ and $\sigma = 0.5$ (Boyd et al., 2011).

4.2 Theoretical approximation

As a first approach, an optimization using a theoretical approximation of the objective function is performed, with the idea of having a theoretical framework (though rough) to further compare and validate the results obtained later with the PowerFactory approach.

4.2.1 Model

The output power profile of each WEC is approximated by a sinusoidal signal with a period equal to the peak period T_p and an average value (and amplitude) equal to the average power of the original profile P_{mean}, as seen in equation 4.1.

$$P(t) = P_{mean} \cdot \left(1 + sin(\frac{2\pi}{T_p}[t - t_{di}])\right) \tag{4.1}$$

where $P(t)$ is the instantaneous power output, and t_{di} is the random time delay commented in Chapter 2.

The sinusoidal output power profile can be observed in Figure 4.1.

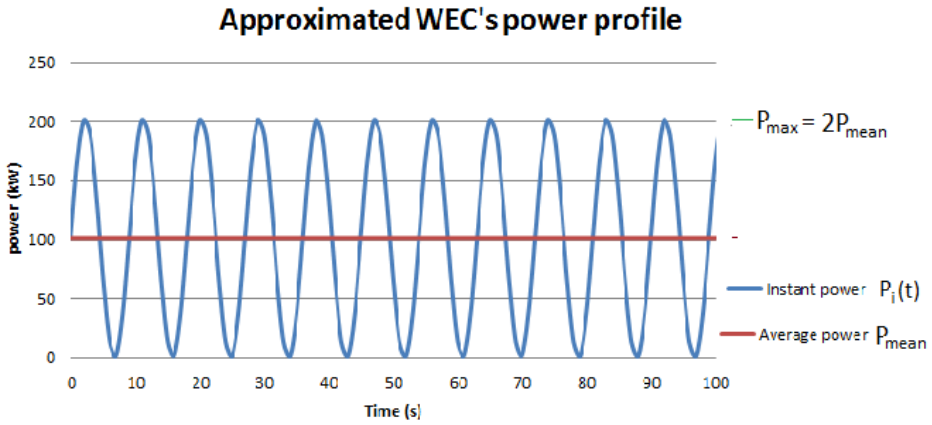

FIGURE 4.1: Power variations in a study-case power profile of a wave energy converter.

When storage is included, equation 4.1 is rewritten as:

$$P(t) = K \cdot P_{mean} \cdot \left(1 + sin(\frac{2\pi}{T_p}[t - t_{di}])\right) \frac{1}{1 + \omega \cdot \tau_i} \tag{4.2}$$

where K is the storage cycle efficiency, τ is the time constant of the storage and ω is the frequency of the signal.

Using this power profile, an approximate value of the energy production and power losses is computed, which is all what is needed to compute the objective function. The energy production of a WEC without storage

E_{NS}, is computed by integration of the sinusoidal power profile (equation 4.1) over the study period T as:

$$E_{NS} = \int_0^T P_{mean} \cdot \left(1 + sin(\frac{2\pi}{T_p}[t - t_{di}])\right) dt \tag{4.3}$$

On the other hand, the energy produced by a WEC assuming storage, with a time constant τ_i, is computed in a similar fashion, by integration of equation 4.2 as:

$$E_s(\tau) = K \int_0^T P_{mean} \cdot \left(1 + sin(\frac{2\pi}{T_p}[t - t_{di}])\right) \frac{1}{1 + \omega \cdot \tau_i} dt \tag{4.4}$$

The cost of power fluctuations is computed (as explained in Section 3.3) using equations 3.10 and 3.11, where the term P_n in 3.11 is given by equations 4.1 (no storage) or 4.2 (storage included). The cost of the storage is computed using equation 3.9 (as explained in Section 3.2), as its value is invariant regardless the approach used.

The sinusoidal profile delivers the same energy as the original power profile over the study period, which gives the two signals equivalence in terms of energy. Due to time constraints, a detailed model using a full-Fourier spectral analysis is out of the scope of this project. Hence, the idea to use a sinusoidal approximation as it is the simplest form under which a variable power profile generated by a wave farm can be modeled.

The optimization problem is carried out using two different configurations:

- Configuration A (5 variables): All the WECs in the same column in the array use the same time constant. This leads to have just 5 different time constants for the five columns of WECs (consisting of 4 WECs each).
- Configuration B (20 variables): Each one of the twenty WECs may have a different time constant.

Figure 4.2 shows the two configurations, to the left the five variable configuration and to the right the individual variables approach.

4.2.2 Results

The sinusoidal power profile was implemented in the cost function of the Neldear-Mead optimization algorithm. A summary of the results is presented in Table 4.1.

TABLE 4.1: Neldear-Mead results using the theoretical-sinusoidal approximation of the power profile.

.	5 variables	20 variables
Number of iterations	290	1000
Time per iteration(ms)	0.84	1.33
Best sample	[0,6 1,5 2,1 2,7 3,1]	Not converged
Annual increase of profits(€)	12056	-

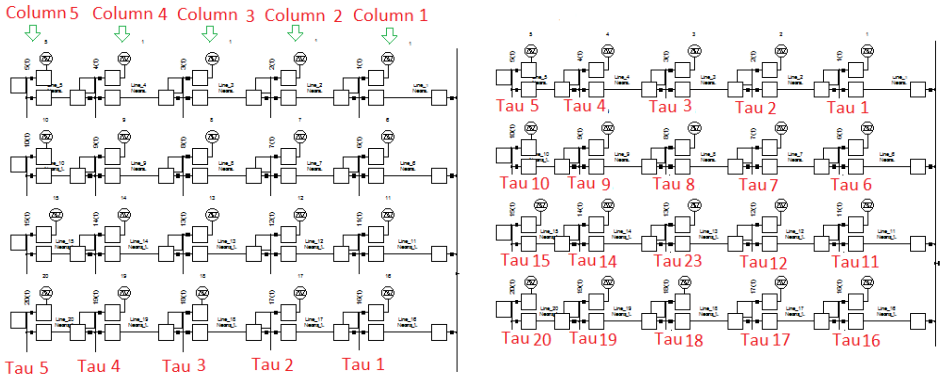

(A) 5 variables configuration; each column of WECs have the same time constant.

(B) 20 variables configuration; the time constant of each WEC is independent of the rest.

FIGURE 4.2: Configurations of five (4.2a) and twenty (4.2b) variables used in the optimization.

The simulations were performed using the parameters presented in Table 4.2.

TABLE 4.2: Basic parameters used in the Neldear-Mead algorithm.

Energy price (€/MWh)	29,5
Number of samples	40
Number of variables	5 / 20
Stop criterion for the algorithm	0,001
Storage efficiency K (%)	96

The values used for the reflection, expansion, contraction and shrink coefficients are: $\alpha = 1$, $\gamma = 2$, $\rho = 0.5$ and $\sigma = 0.5$ as mentioned earlier in Chapter 3.

4.2.3 Discussion of results

Before discussing the results presented in Table 4.1, it is worth to point out the pros and cons of this approximation. The equivalency criteria assumed for this sinusoidal approximation is based on two major facts: first, equal energy delivered over a given period (thanks to equal average power) and second, frequency (or period) of the signal equal to the peak frequency (or peak period) of the original power profile. The first argument seems to be valid as is mandatory to have, at least, the same amount of energy available to deliver. Otherwise, the comparison would be unequal as we would be comparing two signals with different energy contents. However, this assumption should not mislead to think that it is sufficient in itself to achieve accurate results.

In the case of the second equivalence criteria, the peak period T_p represents the period corresponding the maximum energy density of the sea-state, as explained in Chapter 1. However T_p does not represents the totality of the waves, which might lead to differences between both approaches.

Moreover, the original power profile is not periodic, then the fact of modeling it with a periodic signal is itself an approximation. The amplitude of the original profile is also variable, then the effect over the Joule losses is variable as well, which could lead to differences in the final energy delivered to the grid. These differences are more noticeable in Figure 4.3.

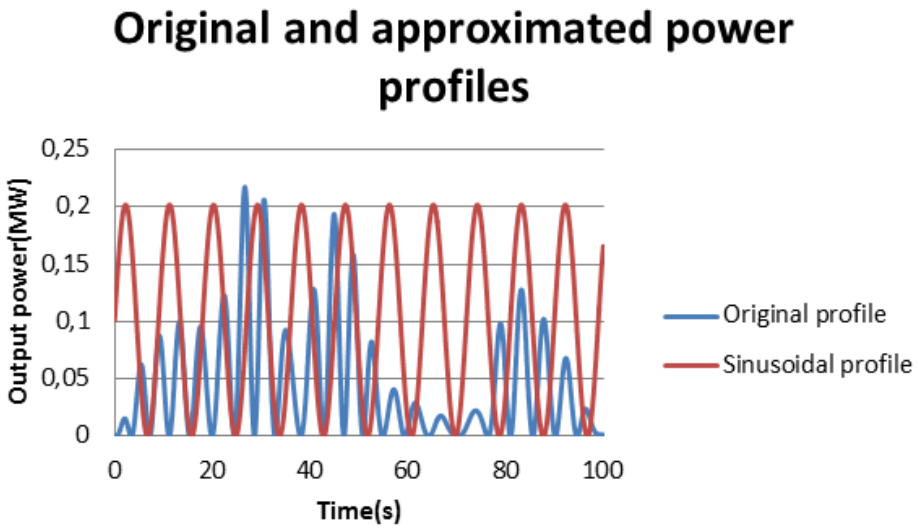

FIGURE 4.3: Superposition of the original and the approximated power profiles in a 100s period.

However, this first approach (using configuration A) helps to confirm some hypothesis presented previously in Chapter 2, about the influence of the position of the WECs in the array over their time constants. As proposed in Chapter 2, one can expect that the optimal capacity of the storage (given by its time constant) increases as the WEC is further from the PCC. WECs in the first column (see Figure 4.2), have a smaller optimal time constant; this value increases as one moves to the fifth column in the array (the furthest from the PCC). This suggests that, it pays off better to place storage with a bigger time constant in columns four and five than in the rest of the columns of the array. This is not exactly the case according to the results obtained using the PowerFactory approach, as will be shown in Section 4.3.3.

Another important point to note, is that a positive result for the cost function was obtained. This means that, according to this theoretical approximation, there is actually an increase on the annual profits of the farm if storage is used. That is the second hypothesis made in Chapter 2 that would be confirmed by these results.

Linked to this, another proposition made, based on the graphics presented in Chapter 2, was that most of the effect of the storage over the losses was for time constants with values less than 5 seconds. Even when no restriction (in terms of the maximum value allowed for the time constant) was used during the optimization, the results yielded values of time constants below 5 seconds.

As stated in Table 4.1, the optimization using the configuration B (20 optimization variables, each WEC having a different time constant) did not converge in 1000 iterations. Several runs were performed but the algorithm was never able to reach a positive value for the objective function and never

reached the convergence in the allowed number of iterations. The reasons for this lack of convergence are still unknown and to be analyzed.

A side achievement of this section is the correct implementation of the Nelder-Mead optimization algorithm in Python, which is important as it is used to perform the optimization in the PowerFactory approach. An example of the evolution of its convergence criteria is shown in Figure 4.4 for the 5 variable configuration.

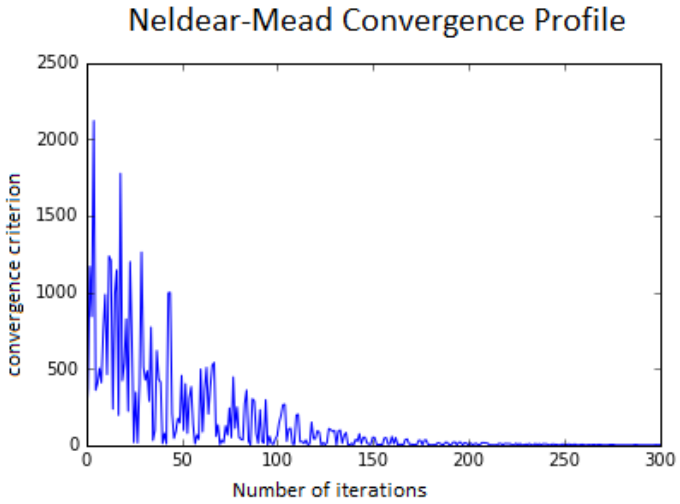

FIGURE 4.4: Evolution of the convergence criteria using the Nelder-Mead algorithm implemented in Python.

4.3 Optimization using PowerFactory

This section could be considered the core of the study, as it uses the interface of PowerFactory with a Python script (Nelder-Mead algorithm) to find the optimal size of the storage units in the wave farm. In a similar manner to Section 4.2.2, the results are presented for configurations A and B (5 and 20 variables respectively) as well as the main parameters and assumptions used in the process. An analysis of the results is performed summarizing the most salient conclusions derived from the simulations pointing out also the limitations encountered.

4.3.1 Motivation

The models and algorithms used by PowerFactory in the computation of power flows are designed and optimized for this purpose, then one could expect that its results are more accurate than the ones obtained in Section 4.2. Besides, it is also optimized from a computing-time perspective, being faster to solve power flows and dynamic simulations. Moreover, due to its graphical interface, it is easy to create the model of the electric systems desired, just by placing the components in the layout and setting their parameters. This feature takes more importance in large and complex systems, where obtaining a mathematical model (and solving it) is not straightforward. The graphical interface makes this software easier to use for research

projects involving multidisciplinary teams including lay people in electrical engineering.

However, despite its excellent capabilities for solving power system problems and its interactive graphical interface, PowerFactory does not allow to perform custom optimization; it just includes some basic optimal power flow algorithms. Hence, the need of interfacing it with an external optimization script, so that PowerFactory can take care of the power flows and dynamic simulations while the rest of the script performs the optimization required. The programming language chosen for the script was Python due to the interfacing capabilities that PowerFactory has with this programming language (DIgSILENT, 2012).

4.3.2 Model

The model used in this project (see Figure 2.1), is based on previous studies performed by Blavette et al.(Blavette et al., 2014) (Blavette et al., 2015)). The farm is supplied by four 2km long submarine cables. WECs are equally spaced in each feeder; its working voltage is 2kV. An onshore substation, connecting the point of common coupling (PCC) to the rest of the network through a 2,5 km overhead line, steps the voltage up from 20kV to 38kV. A VAr compensation system, modeled generically as a controlled source of reactive power and located at the point of common coupling, maintains power factor at this node at a fixed value equal to unity. A series reactor, connected in series with a constant AC 38kV voltage source , represents the rest of the national/regional network.

In this study, the effect of device aggregation on the farm power output is modeled by means of random time delays which are applied to each column of WECs (5 variable configuration) or to each WEC (20 variable configuration).

Generators are modeled as controlled current sources (static generators in PowerFactory) where the storage model is also included. They are connected to the network through a fully-rated power electronics interface.

The objective function in this case, is the same used in the previous section (equation 3.1). The difference in this approach is, that the energy terms ($E_S(\tau)$ and E_{NS}) as well as the cost of power fluctuations ($\Delta P_c(\tau)$ and $\Delta P_{c_{NS}}$) are computed based on the results of the dynamic simulations performed in PowerFactory. The cost of the storage is obtained using the same relation used in the theoretical approach that is developed in Chapter 3.

A summary of the parameters used in PowerFactory to perform the simulations is presented in Table 4.3.

TABLE 4.3: Main parameters included in the PowerFactory model

Simulation Parameters	Values
Simulation time (s)	700
Wave peak period Tp(s)	9
Wave significant Height Hs (m)	3
Time delay between WECs (s)	random (0-200s)
Power factor PCC	1

For the sake of equivalence in the simulation conditions, the parameters of the Neldear-Mead algorithm used in this approach are the same as the ones presented in Table 4.2.

4.3.3 Results

A summary of the results of the optimization process is presented in Table 4.4.

TABLE 4.4: Optimization results using PowerFactory

.	5 variables	20 variables
Number of iterations	100	112
Time per iteration (s)	18,44	17,06
Total convergence time (h)	0,51	0,53
Best sample	[2.50 1.90 3.60 3.60 4.20]	[0.0 0.0 3.34 3.77, 4.23, 2.91 3.16 2.51 2.62 4.61 2.54 1.13 4.17 3.67 3.29 3.61 1.84 4.61 3.15 3.92]
Annual increase of profits(€)	12932	13970

A breakdown of the time, that each task of the optimization algorithm takes, is presented in Table 4.5. This is an important point to take into account to evaluate the eventual suitability of this method for larger scale problems. Figure 3.1 shows a diagram that exemplifies the work flow of both, the PowerFactory and theoretical approaches.

TABLE 4.5: Time of execution needed by the different tasks of the optimization process in one iteration.

Task	Time(%)	Dependent on
Dynamic simulation	58.7	number of time steps
Reading results file	40.6	number of time steps
Neldear-Mead algorithm	0.7	number of variables

4.3.4 Discussion of results

Computing times

The first aspect to highlight is the fact that, contrary to results in Section 4.2.2, the algorithm converged with 5 and 20 variables. When optimization was carried out with 20 variables it took 12% more iterations to converge compared with the case when 5 variables were used. The time per iteration when using 20 variables is even less (7.5%) than for the case of 5 variables and the total convergence time is just slightly higher (4%). This throws a clue that the computing time increases in a much slower fashion than the number of variables.

This could have important implications if this method were to be used in bigger farms (with a bigger number of variables), as it is the objective in the short-term. However, if the layout of the farm is varied (i.e. increased

in complexity and number of elements) the time of the dynamic simulation might also change and may have a significant impact on the overall computing time. As seen in Table 4.5, the dynamic simulation accounts for the highest percentage of time per iteration.

From the analysis of the script, it was noted that for each iteration of the Nelder-Mead algorithm, several "calls" to the objective functions are made. By "call" we mean the computation of the cost value of the objective function. Each of this calls implies to perform a dynamic simulation and one reading of the results file. These two processes account for the highest proportion of time during the algorithm, as stated in Table 4.5. Based on an analysis of the script, an approximated relationship to calculate the total computational time of the whole optimization process was developed as:

$$C_{time} \approx 10,4(N_{samples} + \nu \cdot N_{iterations}) \tag{4.5}$$

where a theoretical value of 2 was predicted for the constant ν, however it was experimentally adjusted to a value of 1.6 to fit better the data. C_{time} stands for the total execution time in seconds, $N_{samples}$ is the number of samples chosen for the algorithm and $N_{iterations}$ is the number of iterations required for convergence.

It is important to recall that the factor of 10.4 that multiplies the rest of the terms, depends on the time required by each call to the objective function and has been experimentally retrieved. Then, any change on the system, including a variation on the simulation time (or size of the time steps) will affect this constant having a major impact on the overall computation time. Possible ways to decrease this value are: decrease the number of time steps of the dynamic simulation or reducing the simulation time if considered appropriate. However, it may not always be possible.

Regarding the other terms of equation 4.5, we observe a linear dependency on the number of samples (as a heuristic method, the Nelder-Mead algorithm requires an arbitrary number of samples to iterate). The ideal number of samples can be obtained experimentally, as shown in Figures 4.5 and 4.6. In both figures, it can be noted that the optimal benefit has a peak, for a certain number of initial samples. Increasing this number of samples results in lower optimal values of the objective function along with a higher computational time, hence the importance of determining the optimal value of this parameter in advance. Besides, as the number of variables increase (20 variables configuration), the algorithm seems to be more sensible to the number of samples utilized, as seen in Figure 4.6.

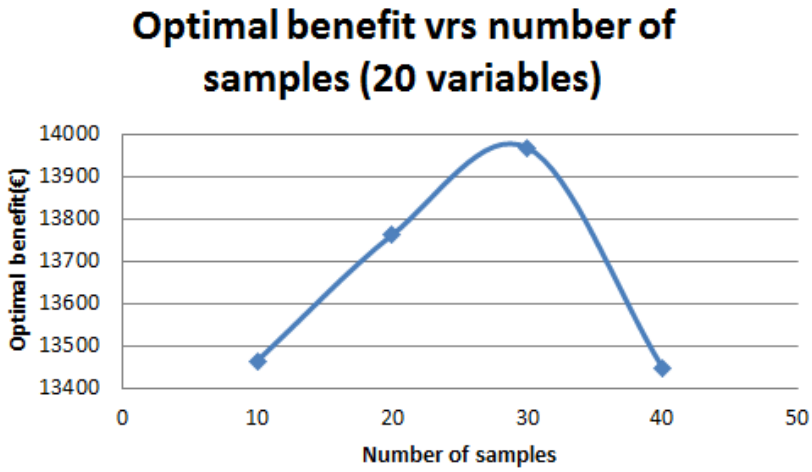

FIGURE 4.6: Experimental estimation of the optimal number of samples for the Neldear-Mead algorithm (20 variables).

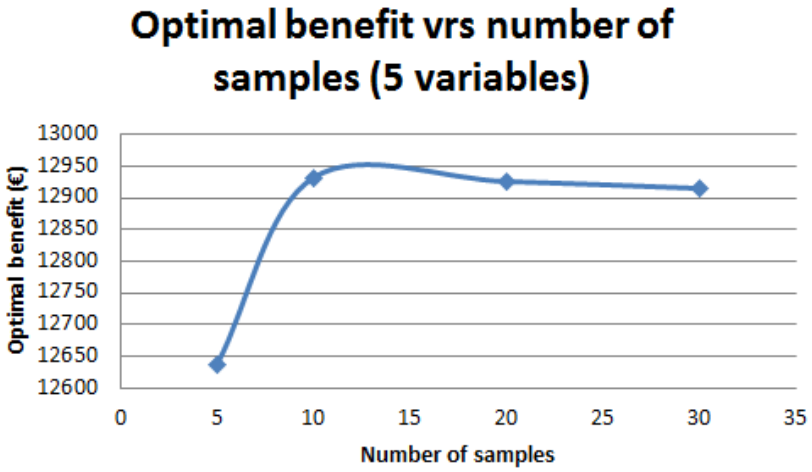

FIGURE 4.5: Experimental estimation of the optimal number of samples for the Neldear-Mead algorithm (5 variables).

The second most influencing aspect over the total execution time is the number of iterations it takes for convergence. This number is never the same, as for any given conditions, the initialization of the algorithm is made by randomly chosen values of the samples. However, results tend to show that this number is related directly with the tightness of the convergence criteria. Then, the value chosen for the convergence criteria has to be as narrow as necessary, according with the accuracy required. Unnecessary iterations derived by a very tight convergence criteria will derive in small improvement of the objective function at the expense of a much higher increase of the convergence time.

It is also important to note that, relation 4.5 is valid for the number of variables (per sample) treated in the present study (< 20). If the number of variables per sample is increased (i.e. in several orders of magnitude) this

experimental relation should be reformulated as, most likely, the number of variables will start playing a role in the computational time.

A person who would like to use this approach in a different and more complex problem, could assess the possibility of using Matlab as scripting language for the optimization script and then compare, if the execution times are better than when Python is used. This due to the fact that, the process of reading the results file of the dynamic simulation in python accounts for 40% of the time per iteration, and tests performed (for other purposes) could suggest that this process might be faster using Matlab.

Optimal time constants

In the case of the configuration A (5 variables), different results were obtained compared to the theoretical approximation, although they share some general characteristics.

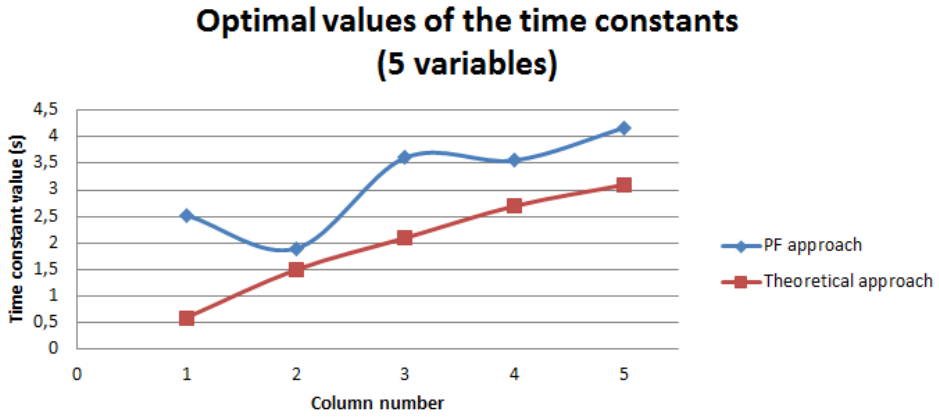

FIGURE 4.7: Comparison of the optimal values for the time constants between the theoretical approximation and the PowerFactory approach (5 variables).

As seen in Figure 4.7, the general tendency of the optimal time constants to increase as the distance from the PCC, is confirmed by the simulations using PowerFactory. Although, not as linear as with the theoretical approximation, the optimal time constants of columns 4 and 5, are clearly higher than the ones of columns 1 and 2. Besides, the values obtained in both cases are in the same order of magnitude.

However, it is clear from Figure 4.7 that, when using PowerFactory, the tendency is not linear; in fact it seems to oscillate as one move away from the PCC. This behavior was consistent over several runs of the algorithm and its cause is not intuitive and remains to be investigated. In the case where the second configuration was used (20 variables), the results of the optimal values of the time constants are presented in Figure 4.8.

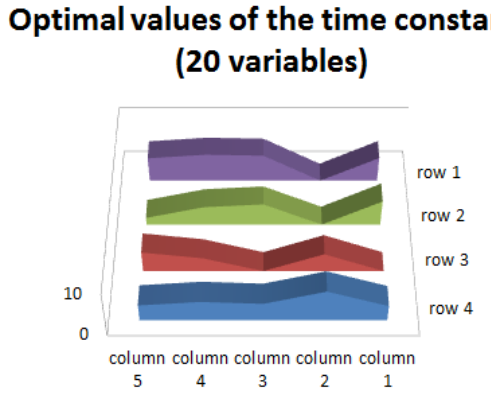

	column 5	column 4	column 3	column 2	column 1
row 4	3,69	4,54	4,08	7,02	3,52
row 3	4,5	3,12	0	4,09	0
row 2	1,61	4,16	4,81	0	5,49
row 1	5,26	6,09	5,87	0	5,32

FIGURE 4.8: Optimal values for the time constants according to the PowerFactory approach (20 variables).

Following the layout of the farm stated in Figure 4.2, the results presented in Figure 4.8 show the values obtained for the time constants after the optimization for each WEC. It is difficult to obtain a tendency of the time constants in this case, because although rows 1 and 2 present a similar behavior, rows 3 and 4 differ completely. If analyzed column-wise, it is also not intuitive to detect any clear tendency. However, if one moves through the columns 1 and 2, the fluctuations of the time constants are sharper than the ones in columns 4 and 5, which coincides with the behavior presented in Figure 4.7. To realize this correlation more clearly, an average value of the time constants per-column was obtained from the results presented in Figure 4.8. This allows to make a column-wise 2-D plot to directly compare the results with the ones obtained in Figure 4.7. This plot is presented in Figure 4.9 where a better correlation (column-wise) is observed between the optimization using 5 and 20 variables.

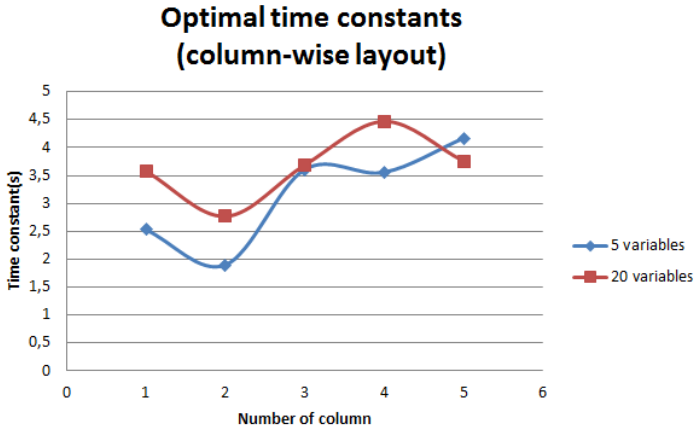

FIGURE 4.9: Column-wise optimal values of the time constants for the 5 and 20 variables configurations (column-averaged values for the 20 variables configuration).

However it has to be noted that, when the optimization was performed with 20 variables, the distribution of the values of the time constants were not coherent throughout the different runs. Different runs yielded totally different distributions of the values of the time constants, then is not possible to generalize the distribution presented in Figure 4.8. However, this distribution was the one that presented the highest increase of annual benefits (the best optimal value), hence the reason why it is presented in this study as the optimal result. It is important to recall that this is a characteristic of any heuristic-based optimization method, the fact of having differences in the results every time the algorithm is run.

However a common point was detected in almost all the runs performed of the algorithm, and it is the presence of zero-values for some storage units, which means that not all the WECs should have storage in order to obtain an optimal value. From both cases (5 and 20 variables), it seems that WECs in column 2 are the least important as they present the smallest values for the time constants while WECs in columns 4 and 5 are the ones that seem to have the biggest effect in the decrease of Joule losses (and increase on farm profits) as they present the highest values in both cases.

Another important point that can be recalled from the results in Table 4.4 is that, the optimization performed over 20 variables (each WEC having an independent time constant), yielded a higher annual increase of profits (8% higher) than the one obtained with the 5 variables configuration.

The proposition of setting all the WECs in each column of the array with the same time constant, came out of a simple assumption. The assumption stays that, as the direction of the waves is considered to be perpendicular to the columns of WECs, every wave would hit all the WECs in a column at the same time. Therefore, their energy production would be equal (so do the Joule losses) as the distance from the point of common coupling is the same for all WECs in the column as well.

Although reasonable, the directional effects may actually appear to have a significant influence which must be taken into account to obtain the globally optimal layout.

4.4 Economical considerations

In this section, a brief analysis from an economical perspective is developed, based on the results obtained. It covers aspects such as the assumptions made for the objective function, the possibility for business as well as alternative solutions to the problem.

4.4.1 Model

A very simple approach has been taken to obtain the cost of the storage, as well as the annual benefits of the farm, according to the objective function (equation 3.1). The assumptions concerning the main financial parameters are presented in Table 4.6.

The storage efficiency value as well as the capital costs for supercapacitors are found in Chapter 1, Tables 1.1, 1.2. Regarding the life expectancy, a conservative value was extracted from the work of Kovaltchouk (Kovaltchouk, 2015). The annual interest rate was taken as a value in the typical

TABLE 4.6: Main economical parameters assumed for the study.

Parameter	Value ✓
Expected life of storage (yrs)	10
Annual interest rate (%)	6
Exchange rate (US $ / €)	1,13
Storage efficiency K (%)	96
Capital cost(supercapacitors) (€/kWh)	1150
Capital cost(supercapacitors) (€/kW)	200
Operation & maintenance (€/year)	Not considered
Aging of storage (% / year)	Not considered

range for renewable energies according to the International Energy Agency (IEA, 2016).

In a formal approach, one should compute the levelized cost of energy (LCOE) of the wave farm, with and without storage. Then, it would require just to compare the values and see which gives the smallest one, and this would say if including storage is economically attractive or not. This approach was not addressed in the present study as it is out of the scope and objectives proposed initially for this project. To develop a comprehensive LCOE calculation of a wave farm is a complete project in itself, and due to time constrains, cannot not be developed in this project.

Instead of using the LCOE, we took only the gross revenues coming from the annual energy production of the farm in both cases: with and without storage, as a reference of the turnover of the farm.

It was tried to determine if placing storage improved the existing level of net income or not. In other words, the main point was to analyze if there was an increase on the net annual income of the farm (product of the sells of the energy produced) after placing optimally sized storage units. This expected increase on net profits was determined accounting for the increase of energy produced by the farm when storage is used (in an annual base) and subtracting the annual cost of this storage.

From this simple parameter it is possible to have an idea of the level of improvement (or not) of placing optimally sized storage units in the farm, without needing to perform a full LCOE analysis. The results are expected to give, at least, a clear idea of the range of values (or percentages) that the owner of a wave farm could expect to see his annual profits increased, if he includes optimally-sized storage in the farm. In this work only two effects of the storage are accounted: increase on energy production and cost of power fluctuations. Any other eventual benefit related to storage (i.e. flicker reduction, voltage regulation) are excluded from this study.

The period used to perform the calculations is one year (T=8760 hours), as most of the economical analysis, including LCOE calculations, are based in annual values, as can be observed in the International Energy Outlook of the EIA (EIA, 2013) or the Projected Costs of Electricity Report of the International Energy Agency (IEA, 2016). The information available about the power generation of a WEC was just for a period of 700 seconds; then this profile was extrapolated to the rest of the year. If a more accurate forecast is desirable, a larger data set of the wave resource should be gathered.

The cost of energy considered throughout this study for all the calculations is $\mathbf{E_c = 29.5\ €/MWh}$. It is chosen as an average wholesale baseload electricity price in France in the first quarter of 2016, as seen in Figure 4.10.

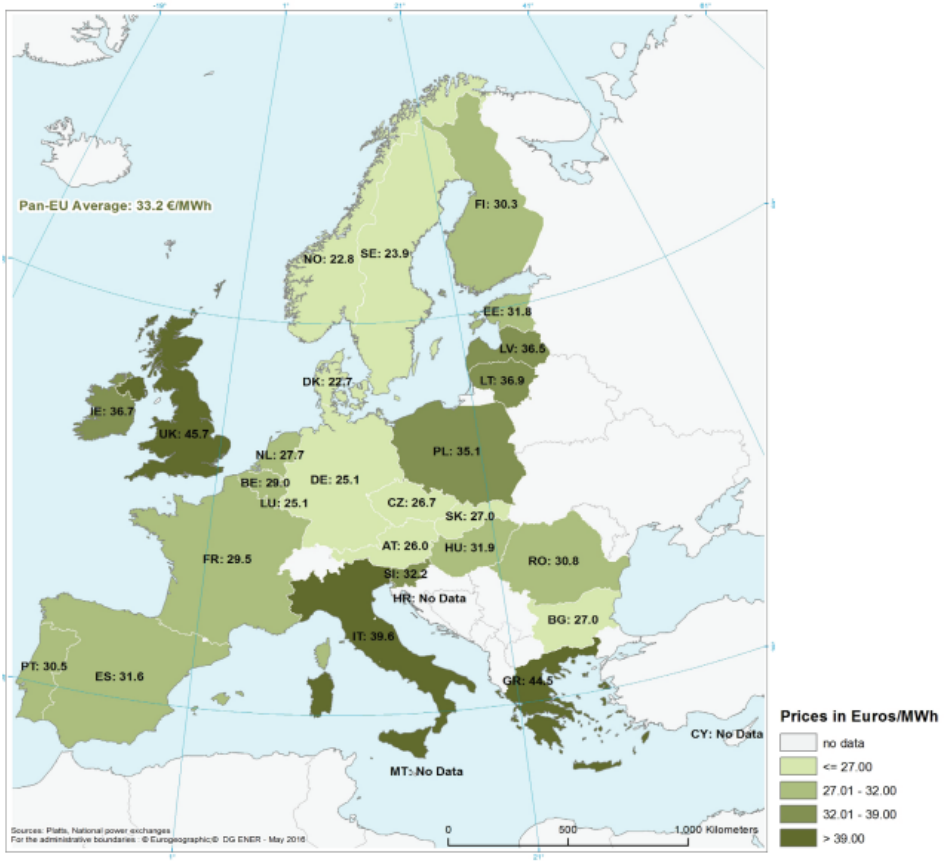

FIGURE 4.10: Comparison of average wholesale baseload electricity prices in different countries in the first quarter of 2016 (IEA, 2016).

4.4.2 Business opportunity

A positive net-increase in annual profits of the farm was found, if optimally sized storage is placed (Table 4.4). The maximum increase of annual profits obtained is around €13970/year (20 variables configuration). This result of course, relies on the assumptions considered for this case study.

The number does not seem to be enough as to create a business out of it, but important points must be addressed where eventual opportunities could arise, that would make storage more attractive for the owner of a wave farm. One of the key points is the cost of power fluctuations. As mentioned in Chapter 3, determining this parameter is rather subjective and depends on particular factors regarding power system type, type of electricity market, type of consumers, governmental regulations, price of energy in the market and so on. A particular combination of these factors could favor the deployment of storage up to the point of being a real business opportunity, while on the other hand, another unfavorable combination could return a decrease on profits if storage is used.

Another aspect found to be crucial, is the storage cycle efficiency. This is definitely one of the most important aspects that need to be researched very carefully in an eventual implementation of storage in a energy production farm. Changes in the range of 10% in storage efficiency provoked variations up to 500% in the increase of profits, which brings to the table another aspect that was neglected in this study: the aging or derating factor of the storage, which is directly linked with the decrease of the cycle efficiency K.

As cycle efficiency has such an important effect in the economic feasibility of storage, then the aging of the storage should be taken into account, over a life-cycle analysis of the farm, to accurately determine whether the inclusion of storage is profitable or not. An annual analysis, as the one performed in this work, is not enough to accurately find out the economic suitability of the storage in the wave farm.

Therefore, from the results obtained in this work, it is difficult to draw a conclusion whether using storage in a wave farm (or other renewable power production plant) will be of advantage in economical terms. Even when the increase in energy production (reduction in Joule losses) were not significant, flicker and voltage regulations in a given country or region could favor (or even force) the use of the storage to be able to comply with such regulations. It would be risky to asseverate whether storage is profitable or not for a wave farm, but what can be said with sufficient certainty is that it definitely has the potential to be profitable and even to become a business opportunity under the correct combination of factors. A particular real-case-study should then be analyzed in detail, taking into account the particular details of location, availability of the resource over the year, size of the project, energy market, energy prices, detailed technical specifications of the equipment, type of consumers, among others; in order to determine whether including storage in the project increase its overall profits (i.e. reduces the LCOE).

4.5 Alternative approaches

As mentioned throughout this document, the purpose of this work is to study the effects of storage on the benefits of a wave farm by reducing the Joule losses, hence hopefully, increasing the energy production. For the purpose of reducing Joule losses, storage has the main drawback of its cycle efficiency which in turn, reduces the energy production as it wastes some of the energy being produced by the WECs.

Therefore, to make the most suitable decision in this regard, it is mandatory to look at other possible solutions to the problem of Joule losses other than placing storage. As it is not the scope of this work, only some alternatives are going to be briefly mentioned in the following paragraphs to arouse the curiosity of someone who would be interested in going deeper in the topic.

Suggestions given by the Research project manager at EdF R&D, Marc LE DU, to tackle this issue are:

- Increasing the size of the cables. The purpose of this idea is to decrease the electrical resistance of the circuit hence proportionally reducing the Joule losses. It is clear that the price of the cables increases

as the diameter increases, yet it is a valid possibility to explore in the assessment process of a renewable energy farm.

- Disconnection of the WECs in periods of peak losses (curtailment). Regarding flicker regulations for instance, it might be viable to disconnect the WECs where fluctuations of the resource are over a certain threshold, that makes flicker exceeding the allowed limits. In other words, instead of trying to directly smooth the power fluctuations, the whole design of the system is developed to allow the disconnection of the system when conditions are extreme. If a sufficient data of the resource is available, it would be feasible to determine, with sufficient accuracy, the percentage of the time when the conditions are going to be extreme, so that the techno-economical analysis can be performed.

  Voluntary curtailment is also being investigated as a solution for derating the cables of wind and wave farms (Sharkey et al., 2011)(Lane, 2011).

In both cases, not only the capital costs of storage would be avoided, but also the installation costs, operation and maintenance costs, extra size and weight in the floating platforms, and so on.

Another "intermediate" solution would be to use equipment, that already has some built-in storage capabilities. The inertial storage capacity of electrical generators for instance, could be sufficient to smooth power fluctuations to an acceptable level. There are many other designs of wave energy converters, that have some degree of built-in storage capacity, which could be used for the purpose at stake. This solution could be worked out in conjunction with an optimal design of the WECs array, to make the most of the aggregation effect (mentioned in Chapter 2).

4.6 Alternating direction method of multipliers

4.6.1 Motivation

One of the initial ideas for this work was to implement a distributed optimization algorithm (ADMM particularly) to compare its performance against a centralized optimization method. This idea emerges from the fact that, many problems in power systems involve a big number of variables, making the optimization process very time consuming.

Distributed optimization algorithms such as ADMM can reduce the computational time by decoupling one problem (with a high number of variables) into several smaller problems whose optimization is simpler, and hopefully faster. If parallel computing is used to solve these simpler problems simultaneously, a significant advantage might be achieved in terms of computational time in some particular problems.

It is expected that real-time optimization capabilities will be required in the near-future by some research projects carried out at SATIE. Hence, it was fundamental to start investigating the advantages and drawbacks of different algorithms of this type.

4.6.2 The method

The algorithm solves problems in the form:

$$\begin{aligned} Minimize &: f(x) + g(x) \\ subject\ to &: Ax + Bz = c \end{aligned} \tag{4.6}$$

with variables $x \in R^n$ and $z \in R^m$, where $A \in R^{p \times n}$, $B \in R^{p \times m}$ and $c \in R^p$. The functions f and g are assumed to be convex.

The method requires to form the augmented Lagrangian as:

$$L_\rho(x, z, y) = f(x) + g(z) + y^T(Ax + Bz - c) + \rho/2\|Ax + Bz - c\|_2^2 \tag{4.7}$$

where ρ is the augmented Lagrangian parameter.

Then, the ADMM consists of the iterations:

$$x^{k+1} := \underset{x}{argmin}\ L_\rho(x, z^k, y^k) \tag{4.8}$$

$$z^{k+1} := \underset{z}{argmin}\ L_\rho(x^{k+1}, z, y^k) \tag{4.9}$$

$$y^{k+1} := y^k + \rho(Ax^{k+1} + Bz^{k+1} - c) \tag{4.10}$$

where $\rho > 0$. The algorithm consists of an x-minimization step (4.8), a z-minimization step (4.9) and a dual variable update (4.10). The dual variable (y) update uses a step size equal to the augmented Lagrangian parameter ρ. In ADMM, x and z are updated in an alternating or sequential fashion, which accounts for the term alternating direction.

Detailed information about the ADMM method can be found in the work of Boyd et al. (Boyd et al., 2011).

4.6.3 Discussion on the implementation

In the problem at stake, the optimization variables are the time constants of the storage units, which do not have a technical restriction on their values. This means, nothing impedes to "buy" a storage unit of any given storage time constant as long as it is available in the market. The previous studies (on which this work is based) were performed for values of time constants from 0 to 5 seconds just because the effect of the storage (in the reduction of Joule losses) decreases dramatically for values above 5 seconds, as stated in Section 2.1.6. Then it would be reasonable to expect that the optimal values for this parameter would be within this range. This fact, make the model presented in 4.6.2 not suitable to solve the problem, as it requires to have a restriction of the form $Ax + Bz = c$.

As an attempt to get rid of this problem, the option of setting an arbitrary limit to the values of the time constants (restrict them to a finite set of values) was studied. If this attempt were to be adopted, a slight different approach of the ADMM algorithm has to be taken. This reformulation allows to work with a restriction of the type $x \in C$ (where $x \in R^n$ and C is a convex set), instead of the restriction stated in equation 4.6. This variation of ADMM requires to compute the Euclidean projection onto the set

C, which requires the set C to have a well defined boundary surface over which, the projection would be reflected.

A surface in space (i.e. a hyperplane of the form $a_1x_1+a_2x_2+...+a_nx_n = b$) implies a direct relation between the variables (i.e. $x_1, x_2...x_n$). In the problem at stake, the time constants of the storage units are independent variables. Physically speaking, the storage units can be sized independently without taking into account the values of the rest of the units. As the variables are independent, no surface hyperplane can be associated to them, preventing the use of the algorithm.

Even ignoring this fact, the computational time is another factor against the implementation of ADMM in this particular case. It is important to recall that many of the most commonly used optimization algorithms require the computation of derivatives of the objective function. If this function depends on a high number of variables, the computation of the derivatives can become, in some cases, really complex and time consuming. In such case, a decoupling method such as ADMM would most likely help to reduce the computational time, especially if parallel computing is used to solve the decoupled problems.

In the problem we are addressing, there is no need to compute any derivatives, as the Nelder-Mead algorithm just requires the evaluation of the objective function, which is carried out by PowerFactory in this case. As analyzed in Section 4.3.4, the computational time of the algorithm had almost no variance regarding the number of variables. This implies that there would be no gain on decoupling the problem into simpler problems, as the algorithm would require roughly the same time to solve the decoupled problems as the time it took to solve the more complex one.

This basically implies that, as we are not using parallel computing, the total time that the Neldear-Mead algorithm is taking to solve the problem, as it is implemented now (in Section 4.3), would be increased in a factor equal to the number of variables (number of "single-variable optimization problems") multiplied by the total number of iterations that ADMM needs to converge. This makes the implementation of ADMM, in the very particular case of the present work, senseless.

However, in an eventual case of an optimization problem where the computational time were dependent on the number of variables and parallel computing were available, ADMM might definitely decrease the computational time of the optimization process in an important proportion.

Chapter 5

Conclusions

This chapter aims to bundle up the main results and accomplishments of this study. It presents a summary of the points considered as the most relevant outcomes, as well as recommendations for further research.

5.1 Preliminary study on power losses

Based on the model assumed for the storage (supercapacitors being the storage mean considered), the time constant (τ) was found to be proportional to the capacitance (the internal series resistance (ESR) being the proportionality factor).

For an storage cycle efficiency (K) less than 96%, placing storage provokes more losses than "savings" in terms of output power, which in turn reduces the total power output of the farm. Hence, K plays an important role in defining whether placing storage in a wave farm is profitable or not.

Centralized storage has no positive effect in reducing active power losses, while decentralized storage does have an effect that depends on the value of time constant chosen. Values of time constants less than 1 second present the highest reduction on power losses.

5.2 Optimization problem

The term that penalizes the power deviations (ΔP_c), plays an important role in the results of the optimization. When this term was neglected, no positive values of the objective function were encountered after the optimization.

The cost of the storage (S_c), was found to be linearly proportional to the time constant, based on the assumption of a first order low-pass filter model for the storage units.

The different terms of the objective function were treated in an annual basis, as this time period is the most commonly used in economical calculations. However, the output power profile of the WECs, that was used in this study, was given in a 700s basis. This is an approximation that should be addressed to improve the accuracy of the results, as the extrapolation of a 700s power profile over a period of one year might not be sufficiently accurate.

5.3 Optimization

5.3.1 Sinusoidal approximation

The sinusoidal approximation used to model the output power profile of a WEC yielded reasonable results for the 5 variable configuration. The optimal values obtained of the time constants were in the same order of magnitude of the ones obtained with PowerFactory. A greater value of the time constant for WECs in column 5 (compared to WECs in column 1), was also obtained using both approaches. However, for the 20 variable configuration, the algorithm was not able to converge in 1000 iterations using the sinusoidal approximation. The reason of the non-convergence remains to be further analyzed.

5.3.2 Nelder-Mead

Nelder-Mead algorithm, was found to be suitable for the PowerFactory approach as it does not require an explicit objective function to work, but just its evaluation. The evaluation of the different terms of the objective function are obtained from the dynamic simulations performed in PowerFactory.

An important point to take into account, when implementing the Nelder-Mead algorithm, is to avoid re-evaluating the objective function of samples that have been already treated. The results from the evaluation of every sample (performed at the beginning of the algorithm) must be kept in memory, to use them throughout the execution of the algorithm. The objective function must be re-evaluated at each iteration, uniquely for the new sample included in that particular iteration. Re-evaluating the objective function for the totality of the samples at every iteration, was proven to make the execution time up to 90% longer.

Nelder-Mead seems to have an optimal number of initial samples, that yields the best results in the minimum amount of iterations. This value must be found experimentally as it depends on each particular application. In the present study, for the 5 variable configuration, an optimal value of around 10 samples was found, while a value of around 30 samples was encountered for the 20 variables configuration.

5.3.3 PowerFactory

An interface between PowerFactory and Python was successfully developed to perform the optimization process. Most of the functions and elements of PowerFactory can be accessed from the external python script. However, some unexpected limitations were encountered, such as the impossibility to use some python packages (i.e. Numpy) as PowerFactory did not recognized them. In turn, this impeded to write the script in a matrix fashion, making the code more inefficient in terms of computational time. Besides that, the access to the PowerFactory results file had to be done entry-wise, as accessing the data matrix-wise is not possible. This may make the process of reading the results of a dynamic simulation very time consuming, if the number of time steps is "large".

Execution time

In every call that the Nelder-Mead algorithm does to evaluate the objective function, two processes must be performed: the dynamic simulation and reading the results. The first process was found to consume the 60% of the computation time while the latter used the remaining 40%. Besides, for less than 20 variables, the computing time per iteration presented almost no variation with respect to the number of variables. However, the number of iterations required for convergence was slightly higher for the 20 variable case. The total execution time of the algorithm was found to depend mostly on the number of samples and the number of iterations required to converge, the latter being the most significant. In the present case study, an average time of 30 minutes was required by the algorithm to converge.

5.3.4 Optimal time constants

The optimal time constants found using the power factory approach, presented values below 5 seconds, as expected from the preliminary simulations shown in Chapter 2. In the 5 variable configuration, storage units placed in columns 4 and 5 seem to have a greater impact on the energy production of the farm compared to the storage units placed in columns 1 and 2. However, this result is not so obvious in the results obtained using the 20 variable configuration.

In the 20 variable configuration, It is difficult to find a column-wise (or row-wise) tendency regarding the optimal time constants. However, the increase of benefits of the farm was 8% higher for this configuration (compared to the 5 variable one), reaching an annual value of 13970 €.

Including storage in a wave farm proved to reduce Joule losses. However, this did not represent an increase in the energy production of the farm in all cases, as it strongly depends on the cycle efficiency K of the storage units.

5.3.5 Economical considerations

Even when an increase on the annual profits of the farm was obtained, this value (13970 €) is not significant in proportion to the net annual profits of the farm (millions of euros). This makes difficult to declare (based on the results of this work), that placing storage in a wave farm would actually increase the profits of the farm.

5.3.6 ADMM

The ADMM algorithm was found unsuitable for the application addressed in this study, as there was no interdependence between the optimization variables (time constants). This is required by the ADMM algorithm for its implementation. Moreover, there was no need in this study to compute the derivatives of the objective function. That might lead to anticipate that the advantages of decomposition (main advantage of ADMM) would not have been significant in this case. Added to the fact that no parallel computing was available, the implementation of ADMM would have incremented the computation time in a factor equal to the number of variables multiplied by

the number of convergence iterations. The advantages of ADMM are envisaged to be relevant in cases where: there is an interdependence between the variables, the computation time depends on the number of variables, it is required to compute the partial derivatives of the objective function (specially if they are complex) and when parallel computing is available to execute the algorithm.

5.4 Recommendations for further research

Regarding the reduction of Joule losses, the evaluation of alternative options, such as voluntary curtailment or the over-sizing of cables, would be of interest in order to validate the adequacy of storage for this purpose.

It would be interesting to interface PowerFactory with Matlab (instead of Python) to compare the execution times. This with the aim of determining which of the two options is better in terms of computation time. An interface with Matlab would have an extra advantage over the interface with Python, which is the possibility of writing and executing the script matrix-wise which would make the code more efficient.

A more detailed model of the storage would be desirable, including calendar and cycling aging. This would help to increase the accuracy of the results. To model and evaluate other storage means (besides supercapacitors) would also be interesting to find out the most suitable option in both, technical and economical terms.

A complete feasibility study, ideally performed over a real case study, would be desirable. This will allow to have access to more accurate information which in turn would lead to more accurate results. A complete lifecycle analysis including the LCOE calculation (with and without storage) is suggested as the best way to determine, with accuracy, the suitability of including storage in economical terms.

Bibliography

Abbey, Chad and Gza Joos (2007). "Supercapacitor energy storage for wind energy applications". In: *IEEE Transactions on Industry Applications* 43.3, pp. 769–776. URL: http://ieeexplore.ieee.org/xpls/abs_all.jsp?arnumber=4214991.

Abedini, A. and A. Nasiri (2008). "Applications of super capacitors for PMSG wind turbine power smoothing". In: *Industrial Electronics, 2008. IECON 2008. 34th Annual Conference of IEEE*. IEEE, pp. 3347–3351. URL: http://ieeexplore.ieee.org/xpls/abs_all.jsp?arnumber=4758497.

Alcorn, Raymond and Dara O'Sullivan (2013). *Electrical design for ocean wave and tidal energy systems*. Vol. 17. IET.

Beirão, Pedro and Cândida Malça (2011). "Hydraulic power take-off prototype for a wave energy converter". In: *ResearchGate*. URL: https://www.researchgate.net/publication/243961971_Hydraulic_power_take-off_prototype_for_a_wave_energy_converter.

Blavette, A. et al. (2014). "Impact of a Medium-Size Wave Farm on Grids of Different Strength Levels". In: *IEEE Transactions on Power Systems* 29.2, pp. 917–923. ISSN: 0885-8950. DOI: 10.1109/TPWRS.2013.2284513.

Blavette, Anne et al. (2015). "Dimensioning the equipment of a wave farm: Energy storage and cables". In: *Industry Applications, IEEE Transactions on* 51.3, pp. 2470–2478. URL: http://ieeexplore.ieee.org/xpls/abs_all.jsp?arnumber=6994805.

Bollen, Math H. and Irene Gu (2006). *Signal processing of power quality disturbances*. Vol. 30. John Wiley & Sons. URL: https://books.google.fr/books?hl=es&lr=&id=cUCDS1DgEgAC&oi=fnd&pg=PR7&dq=Signal+Processing+of+Power+Quality+Disturbances&ots=eJIiQn2lBw&sig=rEmYbx1xuQGef9Z-5TgHjWNIESg.

Boyd, Stephen et al. (2011). "Distributed optimization and statistical learning via the alternating direction method of multipliers". In: *Foundations and Trends® in Machine Learning* 3.1, pp. 1–122. URL: http://dl.acm.org/citation.cfm?id=2185816.

BSI (2015). *NOMINAL VOLTAGES FOR LOW VOLTAGE PUBLIC ELECTRICITY SUPPLY SYSTEMS*. Tech. rep.

Chen, Haisheng et al. (2009a). "Progress in electrical energy storage system: A critical review". In: *Progress in Natural Science* 19.3, pp. 291–312. ISSN: 1002-0071. DOI: 10.1016/j.pnsc.2008.07.014. URL: http://www.sciencedirect.com/science/article/pii/S100200710800381X.

— (2009b). "Progress in electrical energy storage system: A critical review". In: *Progress in Natural Science* 19.3, pp. 291–312. ISSN: 1002-0071. DOI: 10.1016/j.pnsc.2008.07.014. URL: http://www.sciencedirect.com/science/article/pii/S100200710800381X.

Danielsson, O., M. Eriksson, and M. Leijon (2006). "Study of a longitudinal flux permanent magnet linear generator for wave energy converters". en. In: *International Journal of Energy Research* 30.14, pp. 1130–1145. ISSN:

1099-114X. DOI: 10.1002/er.1209. URL: http://onlinelibrary.wiley.com/doi/10.1002/er.1209/abstract.

DIgSILENT (2012). *DIgSILENT PowerFactory User manual*. Tech. rep.

EIA, US (2013). "International energy outlook 2013". In: *US Energy Information Administration (EIA)*.

Falcão, Antonio (2010). "Wave energy utilization: A review of the technologies". In: *Renewable and sustainable energy reviews* 14.3, pp. 899–918. URL: http://www.sciencedirect.com/science/article/pii/S1364032109002652.

Gonzalez-Longatt, Francisco M. and José Rueda, eds. (2014). *PowerFactory Applications for Power System Analysis*. Power Systems. Cham: Springer International Publishing. ISBN: 978-3-319-12957-0 978-3-319-12958-7. URL: http://link.springer.com/10.1007/978-3-319-12958-7.

IEA (2016). *Projected Costs of Generating Electricity*. Tech. rep.

Kolda, T., R. Lewis, and V. Torczon (2003). "Optimization by Direct Search: New Perspectives on Some Classical and Modern Methods". In: *SIAM Review* 45.3, pp. 385–482. ISSN: 0036-1445. DOI: 10.1137/S003614450242889. URL: http://epubs.siam.org/doi/abs/10.1137/S003614450242889.

Kondoh, J. et al. (2000). "Electrical energy storage systems for energy networks". In: *Energy Conversion and Management* 41.17, pp. 1863–1874. ISSN: 0196-8904. DOI: 10.1016/S0196-8904(00)00028-5. URL: http://www.sciencedirect.com/science/article/pii/S0196890400000285.

Kovaltchouk, Thibaut (2015). "Contributions à la co-optimisation contrôle-dimensionnement sur cycle de vie sous contrainte réseau des houlogénérateurs directs". PhD thesis. École normale supérieure de Cachan-ENS Cachan. URL: https://tel.archives-ouvertes.fr/tel-01206269/.

Lane, Danielle (2011). URL: https://www.thecrownestate.co.uk/media/451005/ei-km-in-gt-grid-012009-round-3-offshore-wind-farm-connection-study.pdf.

Lemofouet, S. and A. Rufer (2006). "A Hybrid Energy Storage System Based on Compressed Air and Supercapacitors With Maximum Efficiency Point Tracking (MEPT)". In: *IEEE Transactions on Industrial Electronics* 53.4, pp. 1105–1115. ISSN: 0278-0046. DOI: 10.1109/TIE.2006.878323.

Luo, Xing et al. (2015). "Overview of current development in electrical energy storage technologies and the application potential in power system operation". In: *Applied Energy* 137, pp. 511–536. ISSN: 0306-2619. DOI: 10.1016/j.apenergy.2014.09.081. URL: http://www.sciencedirect.com/science/article/pii/S0306261914010290.

Maxwell (2015). *Energy Storage and Power Delivery for Wind Turbine Pitch Control*. URL: http://www.maxwell.com/products/ultracapacitors/160v-module.

Mitchell, W. H. (1999). "Sea spectra revisited". In: *Mar. Technol* 4.211227.12.

Multon, Bernard (2013). *Marine renewable energy handbook*. John Wiley & Sons. URL: https://books.google.fr/books?hl=es&lr=&id=yv6cYlKjk5cC&oi=fnd&pg=PP9&dq=marine+renewable+energy+handbook&ots=mhLsIW746V&sig=4dg_19bWvZ2ju25mFQL_Se0ThUs.

Nambiar, Anup et al. (2015). "Optimising Network Design Options for Marine Energy Converter Farms". English. In: URL: http://www.research.ed.ac.uk/portal/en/publications/optimising-network-

design-options-for-marine-energy-converter-farms(2286f7af-0f5c-4e25-aa5c-c9ae8986a8d9).html.

Nelder, J. A. and R. Mead (1965). "A Simplex Method for Function Minimization". en. In: *The Computer Journal* 7.4, pp. 308–313. ISSN: 0010-4620, 1460-2067. DOI: 10.1093/comjnl/7.4.308. URL: http://comjnl.oxfordjournals.org/content/7/4/308.

O. Falcão, António F. de (2007). "Modelling and control of oscillating-body wave energy converters with hydraulic power take-off and gas accumulator". In: *Ocean Engineering* 34.14–15, pp. 2021–2032. ISSN: 0029-8018. DOI: 10.1016/j.oceaneng.2007.02.006. URL: http://www.sciencedirect.com/science/article/pii/S0029801807001011.

Pettersson, Karl and Seppo Tikkanen (2009). "Secondary Control In Construction Machinery - Design And Evaluation Of An Excavator Swing Drive". In: *ResearchGate*, pp. 1–10. URL: https://www.researchgate.net/publication/256095814_Secondary_Control_In_Construction_Machinery_-_Design_And_Evaluation_Of_An_Excavator_Swing_Drive.

Plummer, A. R. and M. Schlotter (2009). "Investigating the performance of a hydraulic power take-off". In: *Proceedings of the 8th European Wave and Tidal Energy Conference, Uppsala, Sweden*. Vol. 710, p. 729735. URL: http://sci-hub.cc/http://www.homepages.ed.ac.uk/shs/Wave%20Energy/EWTEC%202009/EWTEC%202009%20(D)/papers/242.pdf.

Pourmovahed, A. et al. (1988). "Experimental evaluation of hydraulic accumulator efficiency with and without elastomeric foam". In: *ResearchGate* 4.2. URL: https://www.researchgate.net/publication/236368214_Experimental_evaluation_of_hydraulic_accumulator_efficiency_with_and_without_elastomeric_foam.

Rastler, D. (2010). "Energy storage markets, application and value analysis". In: *IEEE PES General Meeting*, pp. 1–3. DOI: 10.1109/PES.2010.5589986.

Santos, M. et al. (2012). "Case study on the benefits of energy storage for power quality enhancement : point absorber arrays". In: *ResearchGate*. URL: https://www.researchgate.net/publication/257305245_Case_study_on_the_benefits_of_energy_storage_for_power_quality_enhancement_point_absorber_arrays.

Sharkey, Fergus et al. (2011). "Dynamic electrical ratings and the economics of capacity factor for wave energy converter arrays". In: URL: http://arrow.dit.ie/engscheleart/167/.

Sullivan, Dara O' et al. (2010). "DYNAMIC CHARACTERISTICS OF WAVE AND TIDAL ENERGY CONVERTERS & A RECOMMENDED STRUCTURE FOR DEVELOPMENT OF A GENERIC MODEL FOR GRID CONNECTION". In: *ResearchGate*. URL: https://www.researchgate.net/publication/261031745_DYNAMIC_CHARACTERISTICS_OF_WAVE_AND_TIDAL_ENERGY_CONVERTERS_A_RECOMMENDED_STRUCTURE_FOR_DEVELOPMENT_OF_A_GENERIC_MODEL_FOR_GRID_CONNECTION_A_report_prepared_by_HMRC-UCC_for_OES-IA_under_ANNEX_III_-Int.

Tribbey, Will (2010). "Numerical Recipes: The Art of Scientific Computing is written by William H. Press, Saul A. Teukolsky, William T. Vetterling, and Brian P. Flannery, and published by Cambridge University

Press,\copyright 2007, hardback, ISBN 978-0-521-88068-8, 1235 pp." In: *ACM SIGSOFT Software Engineering Notes* 35.6, pp. 30–31. URL: http://dl.acm.org/citation.cfm?id=187410.

Wilkins, Arnold, Jennifer Veitch, and Brad Lehman (2010). "LED lighting flicker and potential health concerns: IEEE standard PAR1789 update". In: *2010 IEEE Energy Conversion Congress and Exposition*. IEEE, pp. 171–178. URL: http://ieeexplore.ieee.org/xpls/abs_all.jsp?arnumber=5618050.

Williams, Arthur Bernard et al. (2006). *Electronic filter design handbook*. Sirsi) i9780071471718. URL: https://sci-hub.io/http://www.sidalc.net/cgi-bin/wxis.exe/?IsisScript=SUV.xis&method=post&formato=2&cantidad=1&expresion=mfn=008362.